U.S. Department
of Transportation
**Federal Railroad
Administration**

Influence of Vehicle Induced Loads on the Lateral Stability of CWR Track

Office of Research and
Development
Washington DC 20590

Andrew Kish
Gopal Samavedam
David Jeong

Transportation Systems Center
Cambridge MA 02142

DOT/FRA/ORD-85/03
DOT-TSC-FRA-84-6

November 1985
Final Report

NOTICE

This document is disseminated under the sponsorship of the Department of Transportation in the interest of information exchange. The United States Government assumes no liability for its contents or use thereof.

NOTICE

The United States Government does not endorse products or manufacturers. Trade or manufacturers' names appear herein solely because they are considered essential to the object of this report.

Technical Report Documentation Page

1. Report No.	2. Government Accession No.	3. Recipient's Catalog No.
DOT/FRA/ORD-85/03		PB86 168853

4. Title and Subtitle	5. Report Date
Influence of Vehicle Induced Loads on the Lateral Stability of CWR Track	November 1985
	6. Performing Organization Code: DTS-76
7. Author(s) Andrew Kish, Gopal Samavedam*, and David Jeong	8. Performing Organization Report No.: DOT-TSC-FRA-84-6
9. Performing Organization Name and Address: U.S. Department of Transportation, Research and Special Programs Administration, Transportation Systems Center, Cambridge, MA 02142	10. Work Unit No. (TRAIS): RR419-R4304
	11. Contract or Grant No.
12. Sponsoring Agency Name and Address: U.S. Department of Transportation, Federal Railroad Administration, Office of Research and Development, Washington, D.C. 20590	13. Type of Report and Period Covered: FINAL REPORT, January 1983-March 1984
	14. Sponsoring Agency Code: RRD-10

15. Supplementary Notes

*Foster-Miller, Inc.
350 Second Avenue
Waltham, MA 02154

16. Abstract

Thermal buckling of railroad tracks in the lateral plane is an important problem in the design and maintenance of continuous welded rail track (CWR). The severity of the problem is manifested through the increasing number of derailments which are attributable to track buckling, indicating a need for developing better control on the allowable safe temperature increase for CWR track.

The work reported here is a part of a major investigation conducted by the Transportation Systems Center (TSC) for the Federal Railroad Administration (FRA) on the thermal buckling of CWR tracks in the lateral plane.

In this report, the influence of vehicles on the stability of CWR track subjected to temperature rise is examined. The changes in lateral resistance distribution due to vehicle loads are theoretically computed and the buckling response of tracks due to temperature increase is determined for various length cars. It is found that the dynamic buckling temperature for tangent tracks under long cars can be significantly lower than the static buckling temperature, whereas the safe temperature increase values do not appreciably differ. Curved tracks with low lateral resistance can buckle progressively in the presence of long cars, whereas statically (without-vehicle), they may exhibit safe temperature and buckling temperature values.

17. Key Words	18. Distribution Statement
Track Buckling, Track Lateral Stability Dynamic Buckling, Buckling Analysis, Continuous Welded Rail (CWR).	Document is available to the public through the National Technical Information Service, Springfield, VA 22161

19. Security Classif. (of this report)	20. Security Classif. (of this page)	21. No. of Pages	22. Price
Unclassified	Unclassified	94	

Form DOT F 1700.7 (8-72) Reproduction of completed page authorized

PREFACE

Under the Federal Railroad Administration's (FRA) Track Safety Research Program, the Transportation Systems Center (TSC) is conducting research to develop the engineering basis for more effective track safety guidelines and specifications. The intent of these specifications is to ensure safe train operations while allowing the industry maximum flexibility for cost-effective track engineering and maintenance practices.

One of the major safety issues currently under investigation under this program deals with track buckling. The work reported here is part of this investigation and deals with the analytical prediction of critical buckling loads and temperatures of continuous welded rail (CWR) tracks in the presence of vehicle induced loads. Earlier activities under this program entailed analytic and experimental investigations of the static buckling phenomenon.

METRIC CONVERSION FACTORS

Approximate Conversions to Metric Measures

Symbol	When You Know	Multiply by	To Find	Symbol
LENGTH				
in	inches	*2.5	centimeters	cm
ft	feet	30	centimeters	cm
yd	yards	0.9	meters	m
mi	miles	1.6	kilometers	km
AREA				
in^2	square inches	6.5	square centimeters	cm^2
ft^2	square feet	0.09	square meters	m^2
yd^2	square yards	0.8	square meters	m^2
mi^2	square miles	2.6	square kilometers	km^2
	acres	0.4	hectares	ha
MASS (weight)				
oz	ounces	28	grams	g
lb	pounds	0.45	kilograms	kg
	short tons (2000 lb)	0.9	tonnes	t
VOLUME				
tsp	teaspoons	5	milliliters	ml
Tbsp	tablespoons	15	milliliters	ml
fl oz	fluid ounces	30	milliliters	ml
c	cups	0.24	liters	l
pt	pints	0.47	liters	l
qt	quarts	0.95	liters	l
gal	gallons	3.8	liters	l
ft^3	cubic feet	0.03	cubic meters	m^3
yd^3	cubic yards	0.76	cubic meters	m^3
TEMPERATURE (exact)				
°F	Fahrenheit temperature	5/9 (after subtracting 32)	Celsius temperature	°C

*1 in. = 2.54 cm (exactly). For other exact conversions and more detail tables see NBS Misc. Publ. 286, Units of Weight and Measures. Price $2.25 SD Catalog No. C13 10 286.

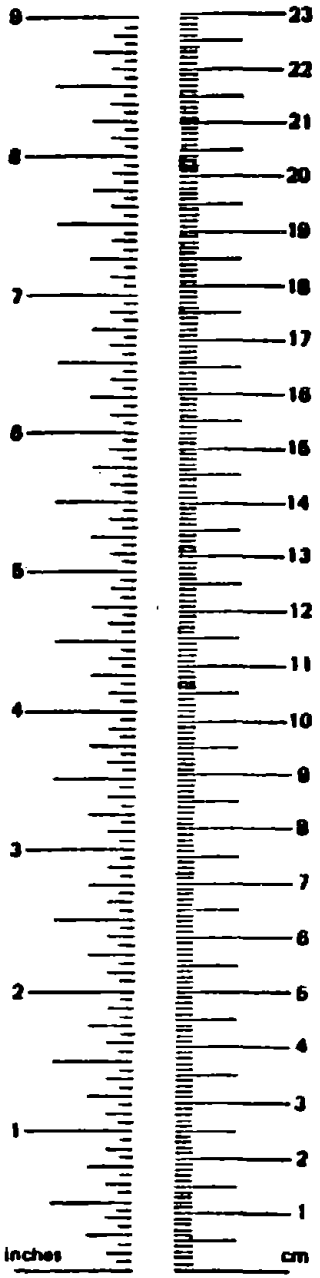

Approximate Conversions from Metric Measures

Symbol	When You Know	Multiply by	To Find	Symbol
LENGTH				
mm	millimeters	0.04	inches	in
cm	centimeters	0.4	inches	in
m	meters	3.3	feet	ft
m	meters	1.1	yards	yd
km	kilometers	0.6	miles	mi
AREA				
cm^2	square centimeters	0.16	square inches	in^2
m^2	square meters	1.2	square yards	yd^2
km^2	square kilometers	0.4	square miles	mi^2
ha	hectares (10,000 m^2)	2.5	acres	
MASS (weight)				
g	grams	0.035	ounces	oz
kg	kilograms	2.2	pounds	lb
t	tonnes (1000 kg)	1.1	short tons	
VOLUME				
ml	milliliters	0.03	fluid ounces	fl oz
l	liters	2.1	pints	pt
l	liters	1.06	quarts	qt
l	liters	0.26	gallons	gal
m^3	cubic meters	36	cubic feet	ft^3
m^3	cubic meters	1.3	cubic yards	yd^3
TEMPERATURE (exact)				
°C	Celsius temperature	9/5 (then add 32)	Fahrenheit temperature	°F

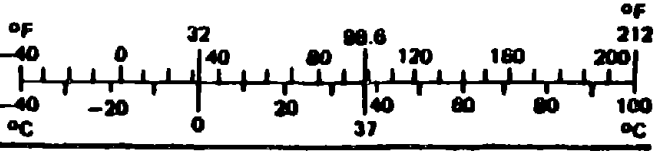

TABLE OF CONTENTS

LIST OF FIGURES

LIST OF FIGURES (continued)

LIST OF FIGURES (continued)

LIST OF TABLES

LIST OF SYMBOLS

x	longitudinal distance from center of track
E	Young's modulus for rail steel
A	rail cross sectional area
I	rail area moment of inertia about vertical axis
ΔT	rail temperature (above the stress-free temperature)
ΔT_s	safe temperature (above the stress-free temperature)
ΔT_B	buckling temperature (above the stress-free temperature)
$\overline{P}$	rail compressive force in the buckled zone
P	compressive rail force in the rails
P_L	applied lateral force in track resistance test
w	lateral deflection
U	axial displacement in the buckled zone
u	axial displacement in the adjoining zone
v	vertical deflection
w'	primes denote derivatives with respect to x
$\dot{w}$	dots denote derivatives with respect to θ
α	coefficient of thermal expansion
F_o	constant lateral resistance
f_o	constant longitudinal resistance
2ℓ	test track length
$2L$	buckling length
$2L_o$	length of misalignment
δ_o	misalignment amplitude
k_v	track modulus (units: lb/in/in abbreviated as psi)
β	PL^2/EI

LIST OF SYMBOLS (continued)

R	radius of curvature
A_m	Fourier coefficient for deflection, w
a_m, b_m	Fourier coefficients as defined in text
ℓ_1	distance between zero longitudinal displacement and center of track
μ	coefficient of friction between ties and ballast
μ_1	stiffness parameter for lateral resistance
L/V	ratio of lateral to vertical load

SUMMARY

The increased utilization of continuous welded rail (CWR) in U.S. railroad tracks has resulted in an increasing number of accidents attributable to derailments induced by thermal buckling of railroad tracks. In an effort to improve the safety of CWR, experimental and analytic investigations are being conducted by the Transportation Systems Center (TSC) supporting the safety mission of the Federal Railroad Administration (FRA). This report describes a part of these investigations dealing with the influence of vehicles on thermal stability of tracks with continuous welded rails and presents results applicable for improved safety, design and maintenance practices.

In this report, principal factors which cause reduction in the lateral resistance of CWR tracks in the presence of vehicles have been identified and quantified theoretically. Buckling response has been determined for tangent and curved tracks under different vehicles including a GP38-2 locomotive and a typical hopper car.

The effect of track vertical stiffness, the coefficient of friction, the influence of single axle and truck L/V, and the effect of truck center spacing on the dynamic buckling strength of CWR track phave been studied. The dynamic buckling and the safe temperature increase results are compared with corresponding values obtained from the static theory (without vehicles). It is shown that for tangent tracks, the dynamic buckling temperatures can be significantly reduced for long cars, but the safe temperature is not appreciably affected. However, for curved tracks with low lateral resistance, buckling can occur progressively in the presence of vehicles. Such tracks statically (without vehicles) may be stable, but may dynamically manifest a progressive response characteristic (i.e. no safe and buckling temperature values). Based on the results of the dynamic buckling analyses, it is concluded that:

1. Vehicle induced influences (such as L/V's and uplift between trucks of long cars) are important in stability analyses and buckling safety considerations.

2. In addition to requirements on allowable safe temperatures and on the control of neutral temperature variation to reduce the potential for buckling, proper safety criteria must include requirements on the dynamic buckling temperature values in order to safeguard against progressive buckling.

1. INTRODUCTION

Thermal buckling of track with continuous welded rails (CWR) has long been a major safety problem for the railroads and the research community. In the United States, the Federal Railroad Administration (FRA) is concerned with the development of the performance based safety specifications for CWR, in order to reduce the numbers of derailments due to thermal buckling. The Transportation Systems Center (TSC) has been supporting the FRA in the development of guidelines and recommendations for improved safety of CWR operations as well as other relevant safety issues.

The research conducted by TSC on track buckling has covered the following major topics:

- o Development of a static theory for the prediction of critical forces and temperatures. The theory assumed that there are no vehicle loads on the track and that the track inertial effects are not important. The buckling plane is considered to be either vertical or horizontal. The horizontal buckling is considered to be more important, although in some situations a three-dimensional mode may also be possible. For a given lateral imperfection, and prescribed lateral and longitudinal resistances, the lateral static stability theory yields a response curve as shown in Figure 1. Critical points on this curve are the buckling temperature increase, ΔT_B, and the safe temperature increase, ΔT_S. Early investigations on the safe temperature increase predictions for tangent tracks by Kerr are available in [1]* and subsequent studies on the buckling temperature increase concept for tangent and curved tracks by Samavedam [2].

* Numbers in brackets denote references

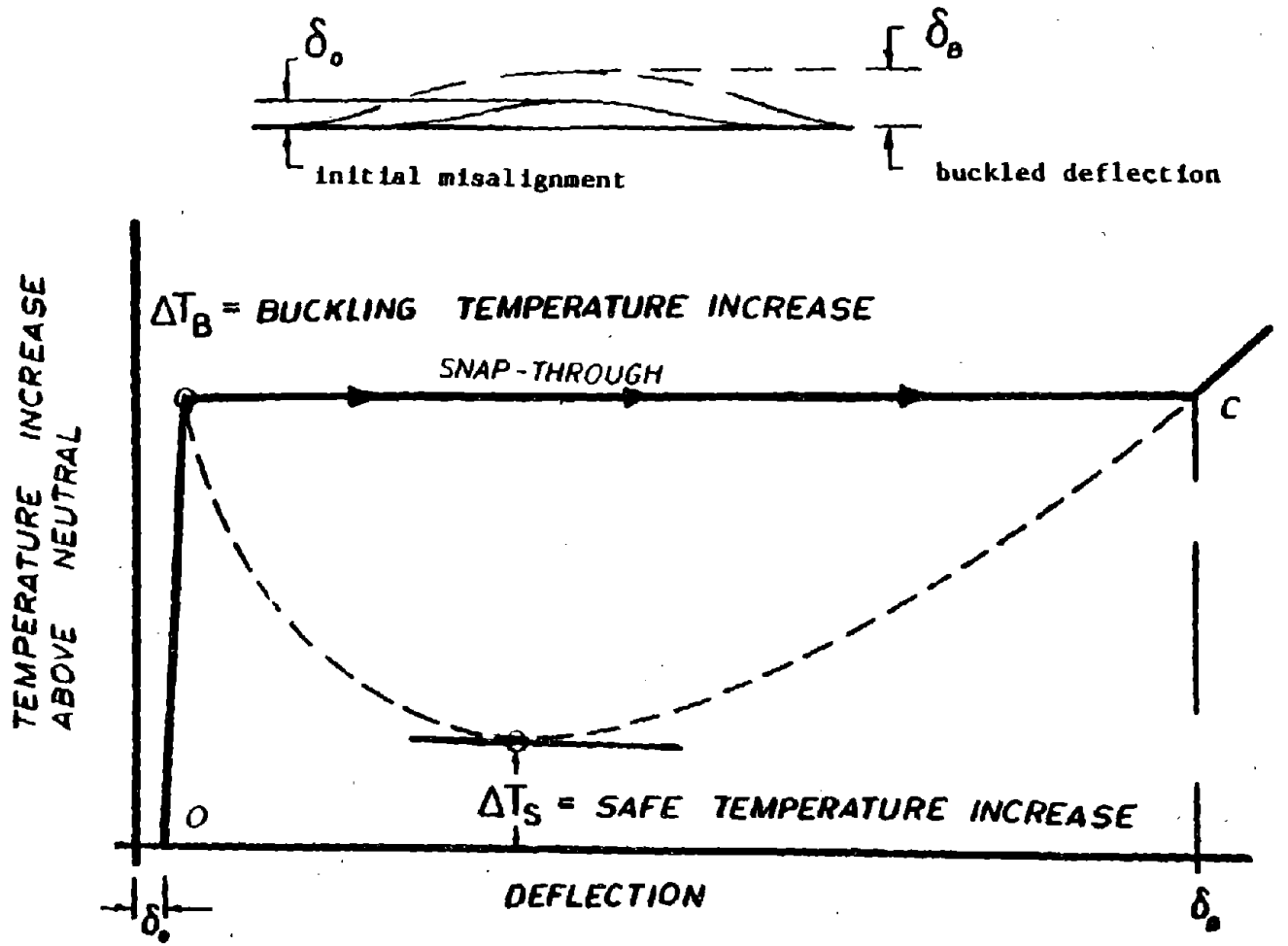

FIGURE 1 - RESPONSE CURVE (STATIC THEORY)

- o Experimental verification of the static theory. The lateral stability theory has been experimentally verified by recent tests [3]. The tests were conducted on a mainline tangent track and 5 degree curved track in June 1981, on the Southern Railway. The rails were heated by passing electric current generated by two GP38-2 locomotives. The test segments were instrumented with strain gages, temperature transducers and longitudinal and lateral displacement transducers. The measured compressive forces, the buckling temperatures and the displacements were compared with the theoretical predictions. Good agreements between the static theory and the experiment have been obtained as indicated in [3].

- o Parametric studies using the static theory. Parametric studies have been performed and the results for buckling and safe temperature increase have been plotted in graphical forms for a range of parameters [4]. The parameters considered are:

  - o Lateral resistance
  - o Longitudinal resistance
  - o Lateral misalignments (amplitude and wavelength)
  - o End stiffness
  - o Length of heated track (finite)
  - o Rail size

A summary of recent investigations of CWR track lateral stability and relevant issues on safety standards in terms of the ΔT_S concept is presented in [5].

The effect of moving vehicles on track lateral stability has not been dealt with so far in the United States, mainly because of the need to validate the simpler static theories before the complex vehicle interaction mechanisms could be sensibly introduced in the analysis. In many European railroad organizations, however, researchers were long concerned with the vehicle induced load effect on CWR track behavior, even before the development of a rational static buckling theory. For example, earlier

Office of Research and Experimentation (ORE) studies attempted to handle "dynamic stability" aspects of CWR tracks by developing a formula for the reduction of buckling strength due to the passage of a vehicle; however, the formula was not derived using a rational theory, nor was it tested against experiments.

Some of the European railroad organizations particularly the French National Railways (SNCF), seem to believe that the majority of track buckles are caused by the passage of vehicles. There is little statistical data to confirm such a claim for U.S. tracks, although, in a recent survey conducted by the Association of American Railroads (AAR) [6], some concern has been expressed in regard to the buckles due to the passage of a train. It appears that a large number (68%) of derailment inducing buckles occurred under the train consist and a few (6%) in front of the locomotive.

In view of the above, the question arises as to what extent dynamic effects and vehicle loads are important in the evaluation of buckling safety. The principal intent of this report is to answer this question theoretically. It is anticipated that once the critical predictions are verified experimentally, useful guidelines can be developed for the safety of track incorporating CWR.

1.1 REVIEW OF LITERATURE

As stated earlier, some of the European railroads have long been concerned with the "dynamic" problem. A notable series of buckling experiments on CWR tangent and curved tracks with and without moving vehicles, were conducted by the Hungarian State Railways [7,8]. The tests without vehicles were called "static buckling tests", and those with moving vehicles were termed "dynamic buckling tests."

The test data from the Hungarian reports, indicate that the vehicle passage on track tends to reduce the buckling safety by about 20-30%. Such a drop is clearly significant and the underlying reasons for this phenomenon have never been explained in the literature.

Different types of dynamic stability tests were carried out by the SNCF [9], using the so called "Wagon Derailleur," which is a device used to exert varying lateral loads for a fixed vertical load on a heated track. The tests simulated varying L/V (lateral/vertical) load ratios. Critical L/V ratios were found to be in the range of 0.67 to 1.15. No further details of the experimental conditions (i.e., track resistances, foundation moduli, etc.) were available. A theory was developed by Ammans and Sauvage [10] to explain the effect of L/V ratio on the lateral distortion of CWR track, but only for small deformations.

Tests simulating lateral and vertical moving loads were performed by the British Rail (BR) in the mid 1970's. Progressive growth of the initial lateral imperfection was monitored for each pass of the vehicle and each increment in the rail temperature. A theoretical analysis of track lateral shift was proposed by C.O. Frederick [11]. In spite of the theoretical and experimental studies on the vehicle effects, the mechanisms relating those effects to a reduction in track buckling strength have not been fully understood. Some of the possible mechanisms that have been hypothesized are:

(i) Uplift of the track due to precession/recession bending wave can cause reduced lateral resistance and hence a reduced buckling strength.

(ii) Lateral forces generated on the track, due to wheel/rail interaction (especially in the presence of lateral imperfections) in combination with many passes of the vehicle, can increase the imperfection's size and, hence, reduce the buckling strength.

(iii) Track vibrations due to the passage of the vehicle can cause loss of lateral ballast resistance due to vibrations being transmitted to ballast. Track vibrations may also reduce the effective bending rigidity (EI) of the rails which can also contribute to some loss of lateral buckling strength.

(iv) Braking and traction forces can also increase compressive forces in the rail.

All these mechanisms need to be examined and theoretically quantified for a realistic assessment and understanding of vehicle effect on lateral buckling strength. The Transportation Systems Center (TSC) has recently initiated work in this direction consisting of:

a) Identification and quantification of the principal influences causing a reduction in the lateral buckling strength of CWR track due to the passage of vehicles through quasi-static and/or dynamic theories.

b) Experimental verification of the "dynamic buckling" theory developed.

c) Incorporation of the vehicle induced effects into a usable safety and design criteria for the prevention of buckling.

The purpose of this report is to provide results relevant to task (a) and present a comparison of static (without vehicle) and dynamic buckling (with vehicle) strengths of CWR tracks. Both tangent and curved tracks will be analyzed. Practical implications of numerical results generated will be discussed. The implication of the present work on track safety standards will be also be given.

2. PROBLEM DEFINITION

In the previous section, the basic aspects relevant to understanding vehicle induced effects on the CWR lateral stability were briefly discussed. In this section, attempts will be made to identify basic problems related to vehicle effects on continuous welded rails subjected to thermal loads.

Figure 2 shows an outline of the elements involved in the analysis of lateral stability of CWR. For completeness, the well developed and experimentally verified static theory is also included. Any theory that explains the influence of a train on the track stability and related phenomena is loosely called the "dynamic theory". In the field of structural mechanics, a dynamic theory of stability implies that there are time dependent disturbing forces acting on the structure, which could lead to a parametric resonance and dynamic instability with deflections growing with time. Such problems have been discussed by Bolotin [12] and their relevance to CWR track will be examined in future studies.

As stated earlier, the static theory is well developed, and has been utilized to conduct parametric studies [4]. Missing from the analysis, however, is the effect of vertical imperfections on the lateral stability of CWR.

A vertical imperfection can result in a lift-off with temperature increase, and consequently, in the loss of some lateral resistance. This could lead to a reduced buckling and safe temperatures in the lateral plane. This phenomenon was alluded to by some of the researchers in the past, but a systematic quantification is not available in the literature. The authors have performed calculations on the subject, and the results will be presented in a forthcoming publication [14]. The analysis developed to study the effect of vertical imperfections on lateral buckling is also useful to study the influence of the precession wave (generated by the trains) on lateral stability.

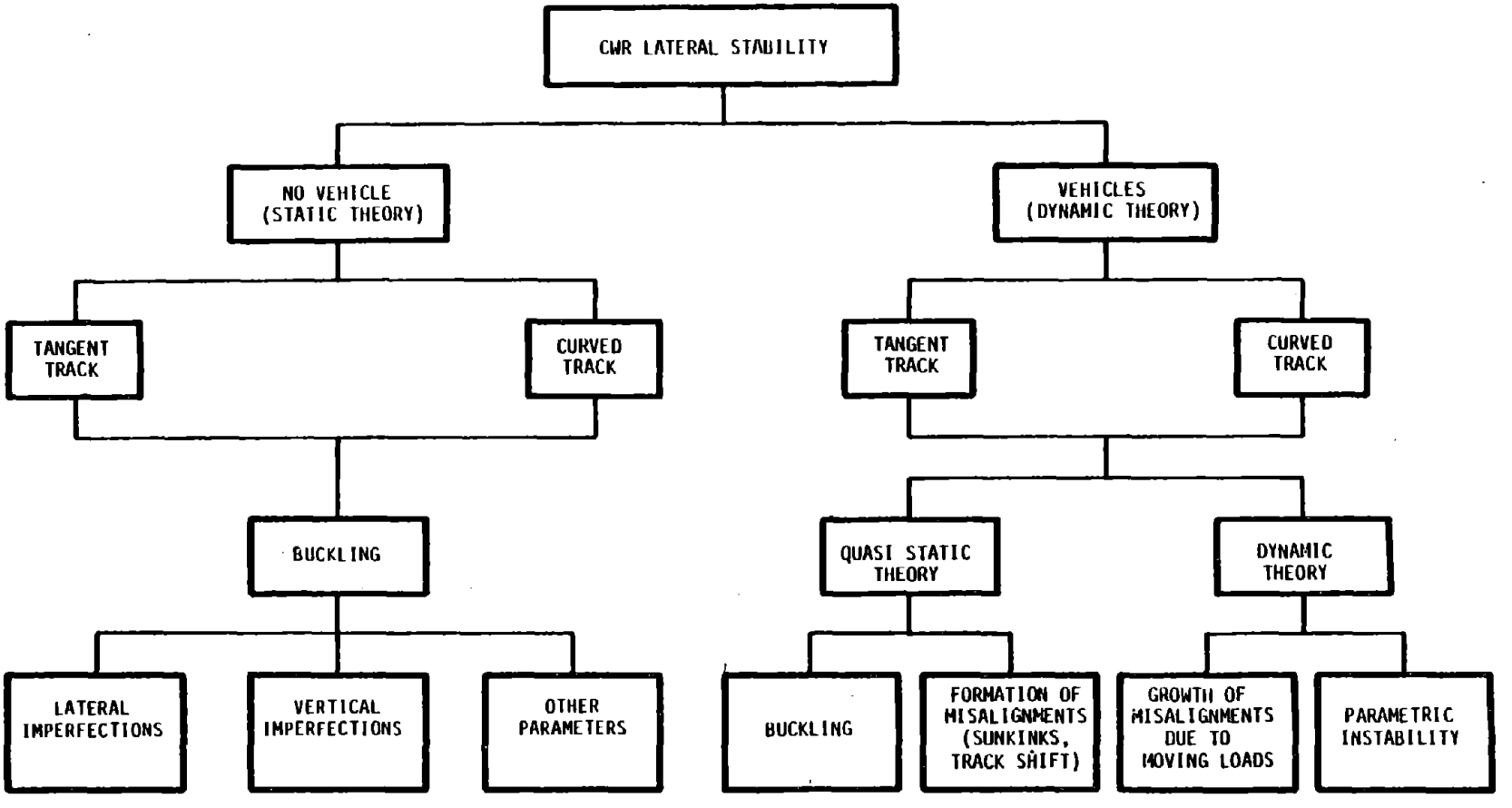

FIGURE 2 - ELEMENTS OF TRACK LATERAL STABILITY

Since the dynamic theory formulations will involve additional terms over those of the static theory, some of the previously derived equations of the static theory will be briefly reviewed here. This will facilitate a better understanding of the more involved dynamic theory.

The starting point in the static theory [2] is the large deflection strain displacement relationship in the buckled zone:

$$e_x = \frac{\partial u}{\partial x} + \frac{1}{2}\left(\frac{\partial w}{\partial x}\right)^2 - \left(\frac{\partial w}{\partial x}\right)\left(\frac{\partial w_o}{\partial x}\right) - \alpha\Delta T \tag{2.1a}$$

The compressive force in the rails is given by:

$$P = AE\, e_x \tag{2.1b}$$

In the foregoing equations, e_x is the total longitudinal strain, A is the cross sectional area of rails, E is Young's modulus, w_o is the lateral (initial) imperfection in the track, u is the axial displacement, w is the additional lateral displacement in the buckled zone, α is the coefficient of thermal expansion and ΔT is the temperature increase over the installation temperature.

Static equilibrium considerations give the following differential equation for the buckled zone:

$$EIw'''' + \bar{P}w'' = F(w) - \bar{P}w_o'' \tag{2}$$

where $\bar{P}$ is the compressive force in the buckled zone (assumed constant), EI is the lateral flexural rigidity (assumed to be the sum of two rails), F(w) is the lateral ballast resistance function, and the primes denote the derivatives with respect to the axial coordinate. Often the lateral resistance function is assumed to be of the form (see Reference 2): $F(w) = F_o \tanh \mu_1 w$. It should be noted that $F(w) = F_o$ (constant) for large μ_1 and $F(w) = (F_o \mu_1)\, w$ (linear) for small μ_1.

FORMULATION FOR VEHICLE EFFECTS

It is convenient to divide the vehicle loads into two classes, namely

- Quasi-Static Loads
- "True" Dynamic Loads

The quasi-static loads are either the steady state loads, or simply some peak values of the transients frozen in time with the inertial effects completely neglected. The dynamic loads contain the time component in some form.

(i) Effect of Quasi-Static Loads on Track Stability

It is assumed that quasi-static load idealization is adequate to explain some of the effects of "uplift" wave, which occurs due to the vertical track deformation under high wheel loads, and possibly due to vertical imperfections and high compressive forces. The fact that wheel loads can produce precession and recession waves; i.e., lift-off of the rail in the front and rear of a wheel which reduces the lateral resistance has been known in the literature for some time, but never been quantified. Also, to date, no acceptable formulation is available to study this effect on CWR track lateral buckling. Therefore, a thorough quantitative examination of this problem has been undertaken in the present report. This examination is referred to as the quasi-static buckling theory with the following assumptions:

- There are constant and known lateral and vertical loads (L and V respectively) per each wheelset (axle).
- The total horizontal load ("truck-lateral") is the net resultant (in the lateral direction) of the two axles. This, in general, may be:
  - (i) the centrifugal force generated while negotiating curves minus the component of wheel load due to superelevation, or
  - (ii) the lateral dynamic force generated due to a lateral imperfection in the track. In this case, the force is strictly a time dependent function. It is assumed

as a constant value in this theory.

- The inertia of the track (both in the longitudinal and the lateral directions) can be neglected.
- The time dependency arising from the speed of the train can be ignored, i.e., the speed of the train is low.

The starting point in this theory is the study of vertical track deformation for the prediction of track uplift. It is assumed, in the vertical deflection analysis, that

- the track has no vertical, initial imperfections
- the effect of thermal force on the vertical deflection is negligible
- the track behaves like a Winkler beam on elastic foundation [13] with a known foundation modulus, k_v
- the inertia forces in the vertical planes are negligible
- there are no vertical oscillating forces in the track.

With these assumptions, the differential equation of equilibrium in the vertical plane can be written as:

$$E_l I_l v'''' + k_v v = \Sigma \delta_i (x-x_i) V_i + Q \qquad (2.3)$$

where $E_l I_l$ = flexural rigidity in the vertical plane
v = vertical deflection
k_v = track foundation modulus
δ_i = Dirac delta functions at appropriate locations of V_i
V_i = vertical wheel loads
Q = track weight per unit length

After solving equation 2.3 subject to the appropriate boundary conditions at infinity, one can determine the distributed foundation (tie/ballast) reaction $R_v(x)$, given by:

$$R_v(x) = k_v v(x) \qquad (2.4)$$

Next it is assumed that the lateral resistance, F, as influenced by vertical loads is given by the Coulomb friction formula:

$$F = F_o + \mu R_v \qquad (2.5)$$

where F_o = lateral resistance without wheel loads and includes the part due to the self weight of the track
μ = tie to ballast friction coefficient.

If R_v happens to be negative (upwards) at a point and is more than the weight of track (per unit length) in magnitude, at that point the lateral resistance is computed differently as discussed in Appendix A.

The values of μ vary with tie and ballast type and condition, and typically range between 0.4 and 0.8. A remark is made that in equation 2.5, the lateral resistance F is assumed to be independent of the lateral displacement w, but is proportional to the vertical displacement v. Since v varies as a function of axial coordinate x, F will also vary axially.

In accordance with the assumptions stated earlier, the equilibrium equation in the lateral direction is

$$EIw'''' + \bar{P}w = -F(x) - \bar{P}w_o'' + \Sigma\delta_i (x-x_i)\, L_i \qquad (2.6)$$

where δ_i are Dirac's delta functions at the appropriate locations of lateral wheel loads L_i.

Equation 2.6 is most conveniently solved by the Fourier technique [2] (also see Appendix B). From the analysis, the response curves are expected to be of similar form to the pure static case.

The values of the buckling and safe temperature increases will be compared with those from the pure static theory in which the vertical deflection v = 0 and the lateral loads $L_i = 0$.

(ii) Formation of Lateral Imperfections

Apart from altering the stability response curve discussed earlier, another important influence which the vehicle loads play on CWR at high

temperatures is to cause formation of track distortions or sunkinks. A theory was proposed in Reference [10] by Ammans and Sauvage, who considered a single wheel and an arbitrarily fixed wavelength of 26.25 feet (8 meters). The formulation given in the previous section is also applicable here, except that the lateral deflections are small and of the order of a few millimeters. Consequently, the "initial" lateral resistance in the function $F(w) = F_o \tanh \mu_1 w$ is to be fully incorporated in the analysis. Although this is not truly a subject of stability, in view of its practical importance, it will be the subject of subsequent studies.

(iii) Growth of Imperfections

A lateral imperfection in the track can grow not only because of the temperature rise, but also due to the wheel passage over the imperfection. While negotiating the imperfection, a lateral dynamic force may be generated, or a reduction in lateral resistance due to lift off can occur. This may push the track to a new equilibrium position, with larger amplitude and wave length of imperfection. The following wheel may exert a lateral force which is dependent on the existing imperfection size and wave-length. (Generally the lateral force increases with the increase in amplitude and decreases with the increase in the wavelength.) If the force developed is less than a critical value (which depends on the ballast lateral resistance, rail compressive force and the lateral dynamic parameters of the track), then there will be no further increase in the imperfection size.

The foregoing phenomenon is quite complicated and the mechanism involved is only marginally understood. A detailed analysis of the imperfection growth and its influence on track stability will be undertaken in a future study. The relevant aspects of the track lateral stability phenomena are summarized in Table 1.

TABLE 1 - TRACK LATERAL STABILITY MECHANISM

STAGE	EVENT	CAUSE
1	FORMATION OF INITIAL TRACK MISALIGNMENTS	(1) REDUCED LOCAL RESISTANCE (2) HIGH L/V'S AND LONGITUDINAL FORCES (3) INITIAL IMPERFECTIONS (WELDS) AND WEAK SPOTS
2	GROWTH OF MISALIGNMENTS	(1) L/V INCREASE DUE TO THE IMPERFECTIONS (2) INCREASE IN LONGITUDINAL FORCES (3) TRACK UPLIFT DUE TO VERTICAL LOADS (4) TRAIN INDUCED VIBRATION
3	BUCKLING	(1) HIGH LONGITUDINAL FORCE (2) REDUCED T_n (STRESS-FREE TEMPERATURE) (3) UPLIFT WAVE (LONG CARS)

3. STABILITY CONSIDERATIONS

As stated in Section 2.0, quasi-static loads are either steady static loads, or simply some peak values of dynamic transients between the vehicle and the track. In the presence of thermal loads these loads can cause track instabilities such as lateral distortions and sunkinks. In this section, lateral instability (buckling) will be examined in detail, while formation and growth of sunkinks will be a subject of future studies.

Calculations for the lateral stability of CWR track under the influence of quasi-static loads due to the passage of a single axle, a single truck and a vehicle with two trucks have been performed. It was assumed that a Shape I type symmetric buckling mode occurs in each of the cases considered.

3.1 SINGLE AXLE: INFLUENCE OF L/V

An initial simplifying assumption is made that the influence of adjacent axles does not spread far enough to interfere with that of the axle under consideration. This assumption is not strictly valid, as seen later from the calculation made for a truck (two axles), however, the problem of the single axle is of basic interest for preliminary considerations. Of particular interest is the case when the wheels exert a lateral load while negotiating a curve at some given speed. The vertical wheel load V tends to stablize the track (at least, under the wheel) whereas the lateral load is expected to reduce the lateral buckling strength. Given the track characteristics and the wheel loads, the problem of practical interest here is the determination of maximum safe speed from the thermal buckling point of view. For high speed trains running in excess of the balance speed for curved tracks, the speed limit on hot summer days is an important consideration, as seen from numerous tests conducted by BR, SNCF and other railroad organizations.

An important parameter in the analysis is the L/V ratio. The vertical load V is due to the weight of the car. The lateral load L can be expressed in terms of weight, the speed, the superelevation and curvature.

It must be remarked that the lateral forces can also be generated from several lateral misalignments, hunting and other dynamic vehicle track interaction mechanisms. It is assumed that all these mechanisms would yield a known quasi-static L/V ratio.

Figure 3.1 shows the vertical deflection profile for a set of the assumed parameters. The deflection is determined using equation 2.3. Details of the solution are presented in Appendix A. Using equation 2.5, the lateral resistance is determined as a function of the axial distance.

Equation 2.6 is used to determine the safe temperature increase as in [2]. Lateral misalignments have not been included. Figure 3.1 shows the assumed mode of buckling in the lateral plane.

Numerical Results: Several numerical computations have been performed for a 5^{o} curve. The effect of curvature in the vertical deflection analysis has been neglected. The parameters are shown in Figure 3.1. The safe temperature increase values are plotted in Figures 3.2 and 3.3.

As seen from these figures, for $L/V < 0.6$, the safe temperature increase values are greater than those for the track without vehicles. This is to be expected because the friction coefficient is taken as 0.6. In general, it can be shown that the critical ratios of L/V which reduce the track lateral buckling strength are equal to or greater than the tie ballast friction coefficient, μ. Hence,

$$(L/V)_{CRIT} > \mu \qquad (3.1)$$

Generally for most tracks $\mu > 0.6$ and $L/V < 0.6$. Therefore, it can be concluded that track lateral stability under the influence of a single wheel may not be a serious problem (special cases such as very tight curves, very high speeds and large initial misalignments excepted).

ASSUMED PARAMETERS

L/V = 0.0 to 0.6

lateral resistance = F_0 = 33.5 lb/in to 55.9 lb/in (600 kg/m to 1000 kg/m)

curvature of 5°

foundation modulus = k_v = 4000 psi

coefficient of friction = μ = 0.6

longitudinal resistance = f_0 = 55.9 lb/in

rail size of 132RE

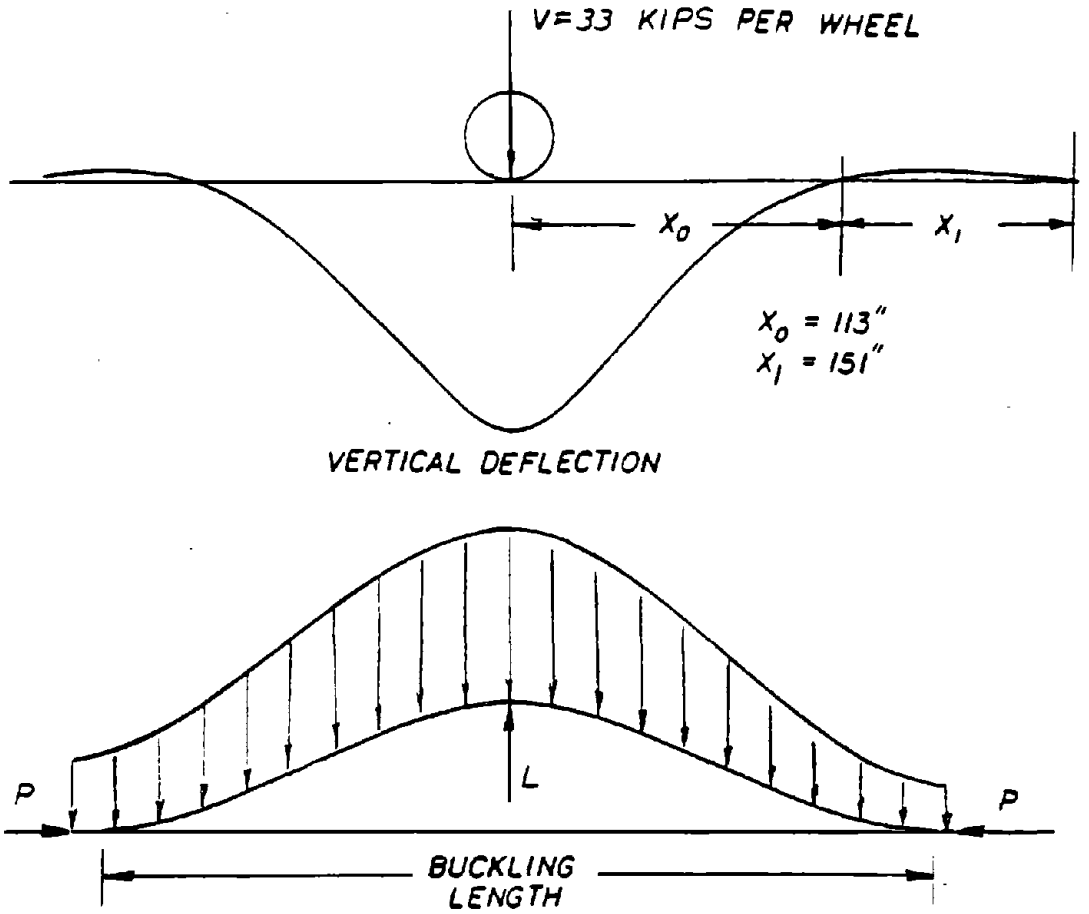

FIGURE 3.1 - FORCES AND DEFLECTIONS OF TRACK UNDER SINGLE AXLE LOAD

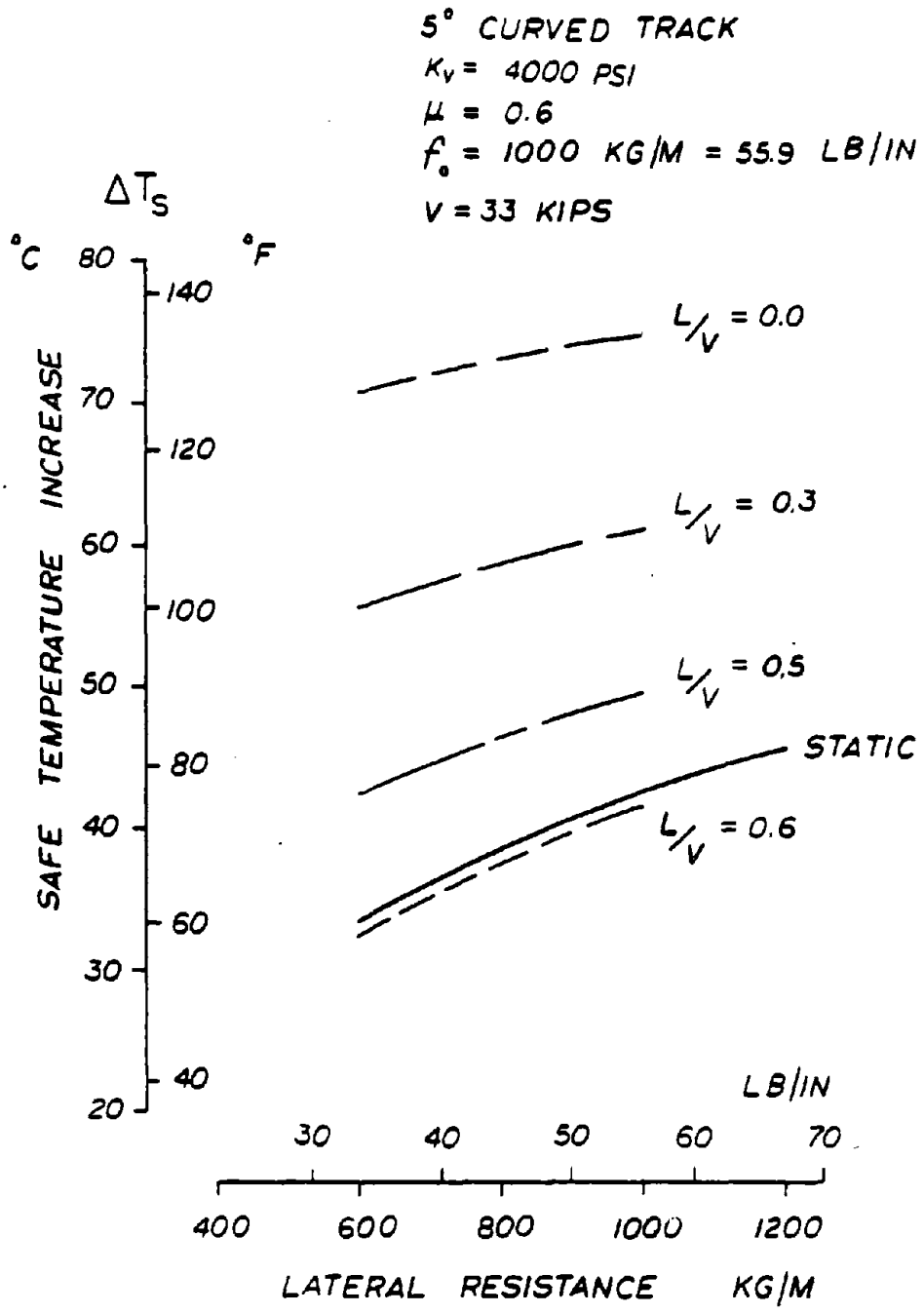

FIGURE 3.2 - SAFE TEMPERATURE INCREASE AS A FUNCTION OF LATERAL RESISTANCE AND L/V RATIO (AXLE LOAD)

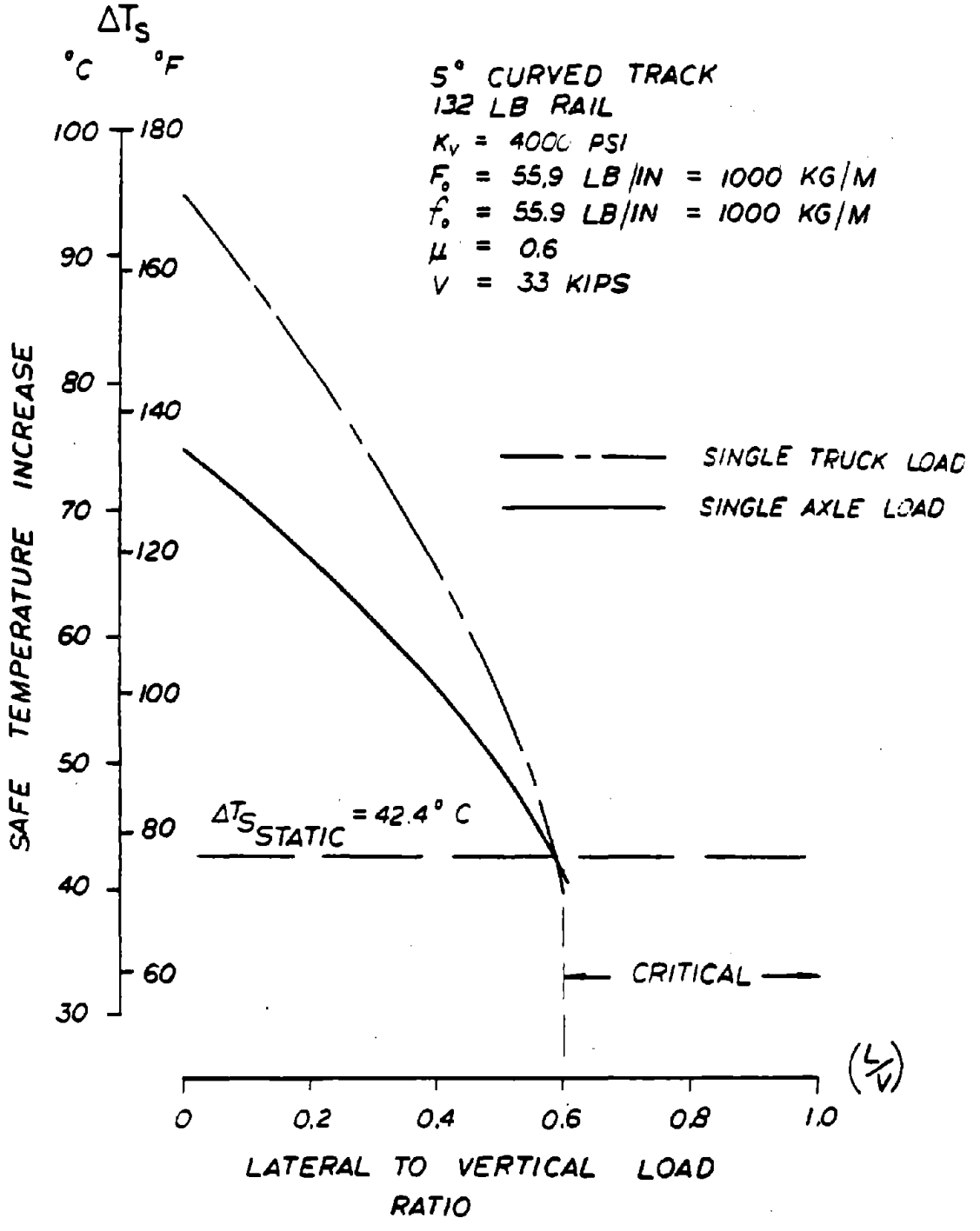

FIGURE 3.3 - EFFECT OF L/V RATIO ON SAFE TEMPERATURE INCREASE (AXLE VERSUS TRUCK LOAD)

3.2 SINGLE TRUCK: INFLUENCE OF L/V

Considering typical two-axle truck configurations, the vertical deflection profile is as shown in Figure 3.4 together with the assumed symmetric buckling mode in the lateral plane.

The parameter of interest is again L/V, and the safe temperature increases have been determined for a range of curvatures. The analysis is similar to the one used for the single axle.

Numerical Results: Figure 3.3 shows the results for the truck (for parameters given in Figure 3.4). Again, the critical L/V is equal to or greater than 0.6, which is the coefficient of friction between the tie and the ballast.

Figure 3.5 shows safe temperature increases for tracks with different lateral resistance values, under the influence of the single truck. It is interesting to note that for lateral resistance less than 1000 kg/m, there is no safe temperature increase for L/V > 0.6. The track continuously shifts with temperature increase. This is referred to as progressive buckling. The implications of the progressive buckling scenario on track safety will be discussed later.

Figure 3.6 shows the safe temperature increases for a range of curvature values from 0^{o} (tangent track) to 7^{o} curve. It is seen that L/V = 0.6 is critical for tracks with curvatures greater than 4 degrees since progressive buckling will occur.

3.3 CAR INFLUENCE: EFFECT OF CENTRAL UPLIFT WAVE

In the previous cases of single axle and single truck, consideration has been given to the lateral wheel loads. If the lateral loads are not present, as it may be for tangent track or curved track with vehicles running at balance speed, then the track is essentially stable under the wheels. In this scenario, buckling modes as assumed in Figure 3.1 and 3.4 are of no practical interest. This is not to imply that lateral loads are

ASSUMED PARAMETERS

L/V = 0.0 to 0.6

lateral resistance = F_0 = 33.5 lb/in to 55.9 lb/in (600 kg/m to 1000 kg/m)

curvature of 0 to 7°
foundation modulus = k_v = 4000 psi
coefficient of friction = μ = 0.6
longitudinal resistance = f_0 = 55.9 lb/in
rail size of 132RE

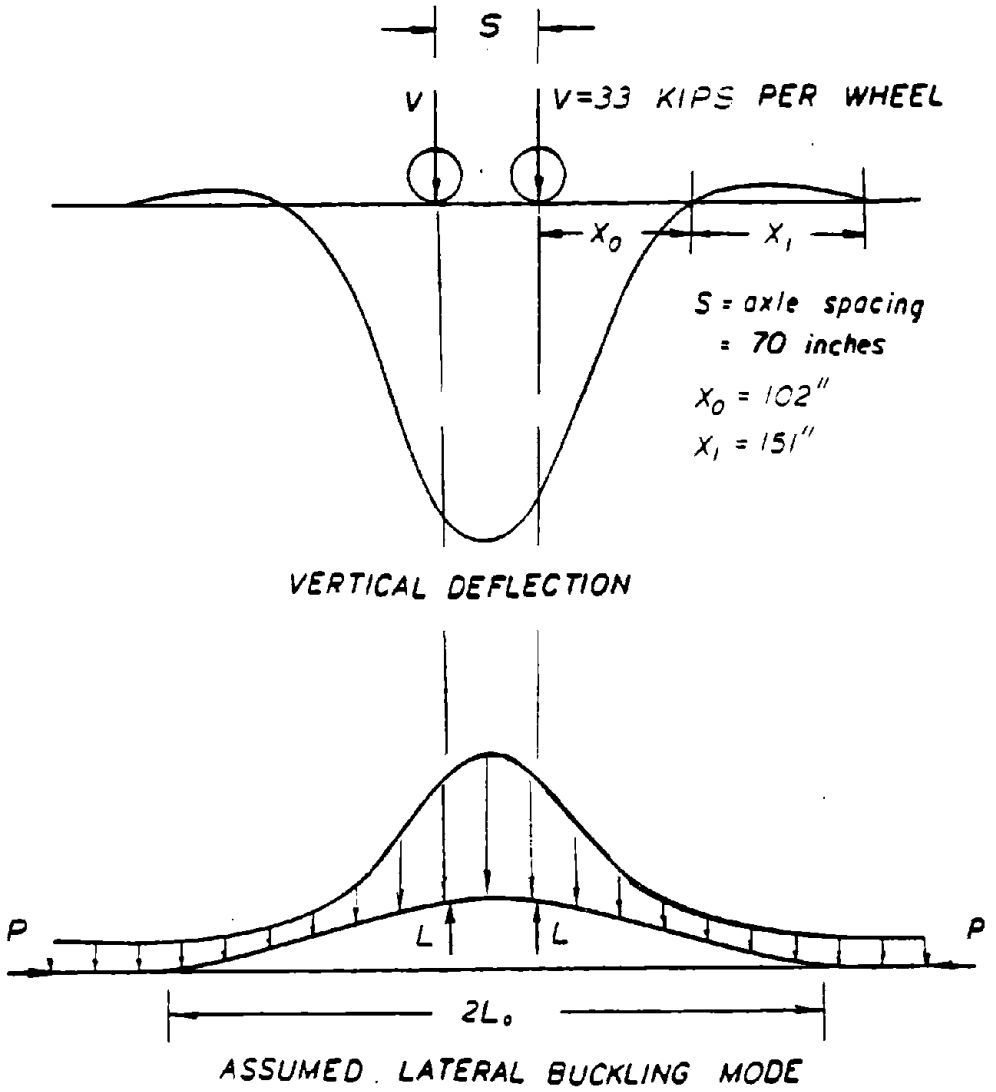

FIGURE 3.4 - FORCES AND DEFLECTIONS OF TRACK UNDER TRUCK LOADS

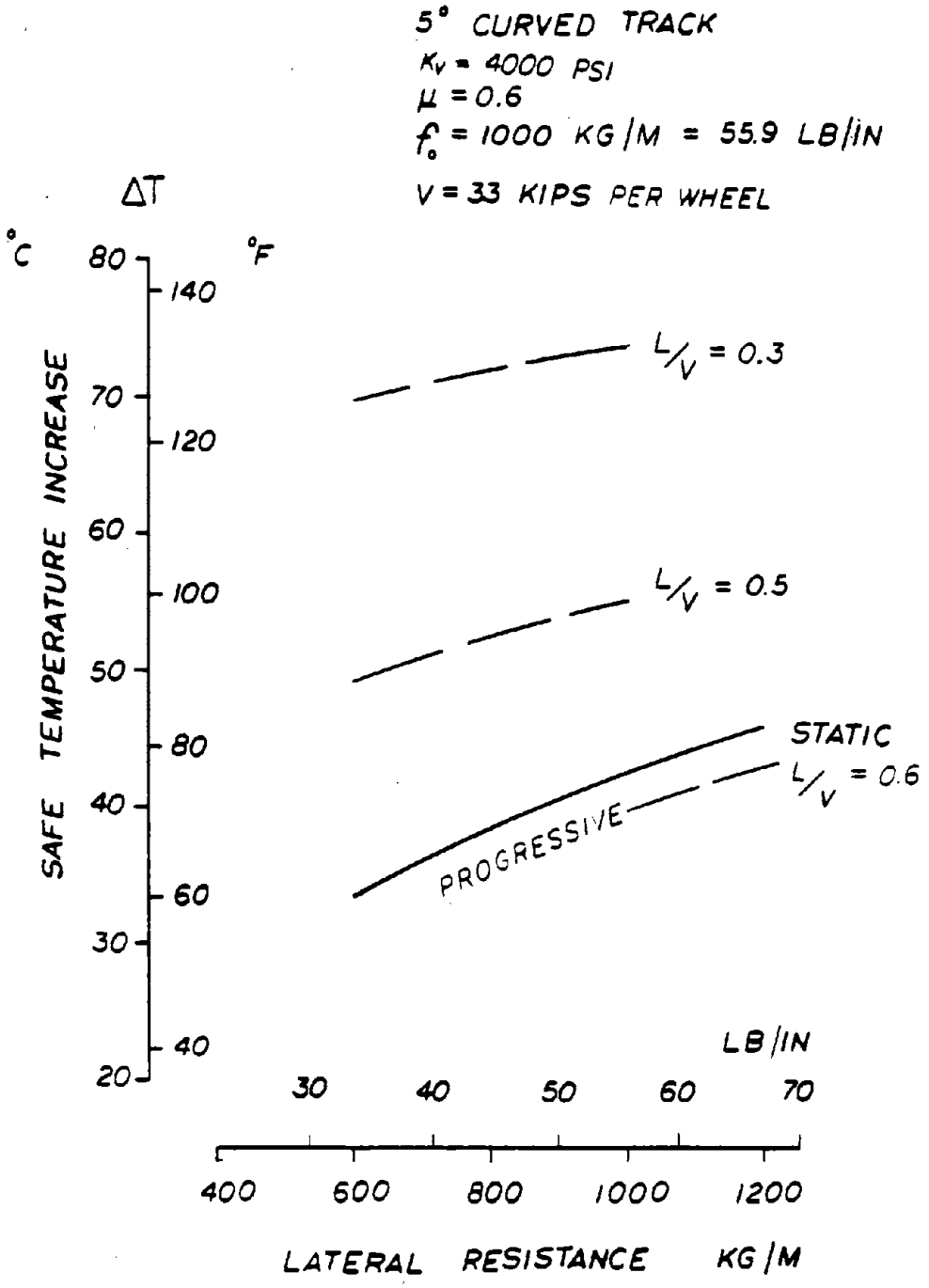

FIGURE 3.5 - SAFE TEMPERATURE INCREASE AS A FUNCTION OF LATERAL RESISTANCE AND L/V RATIO (TRUCK LOAD)

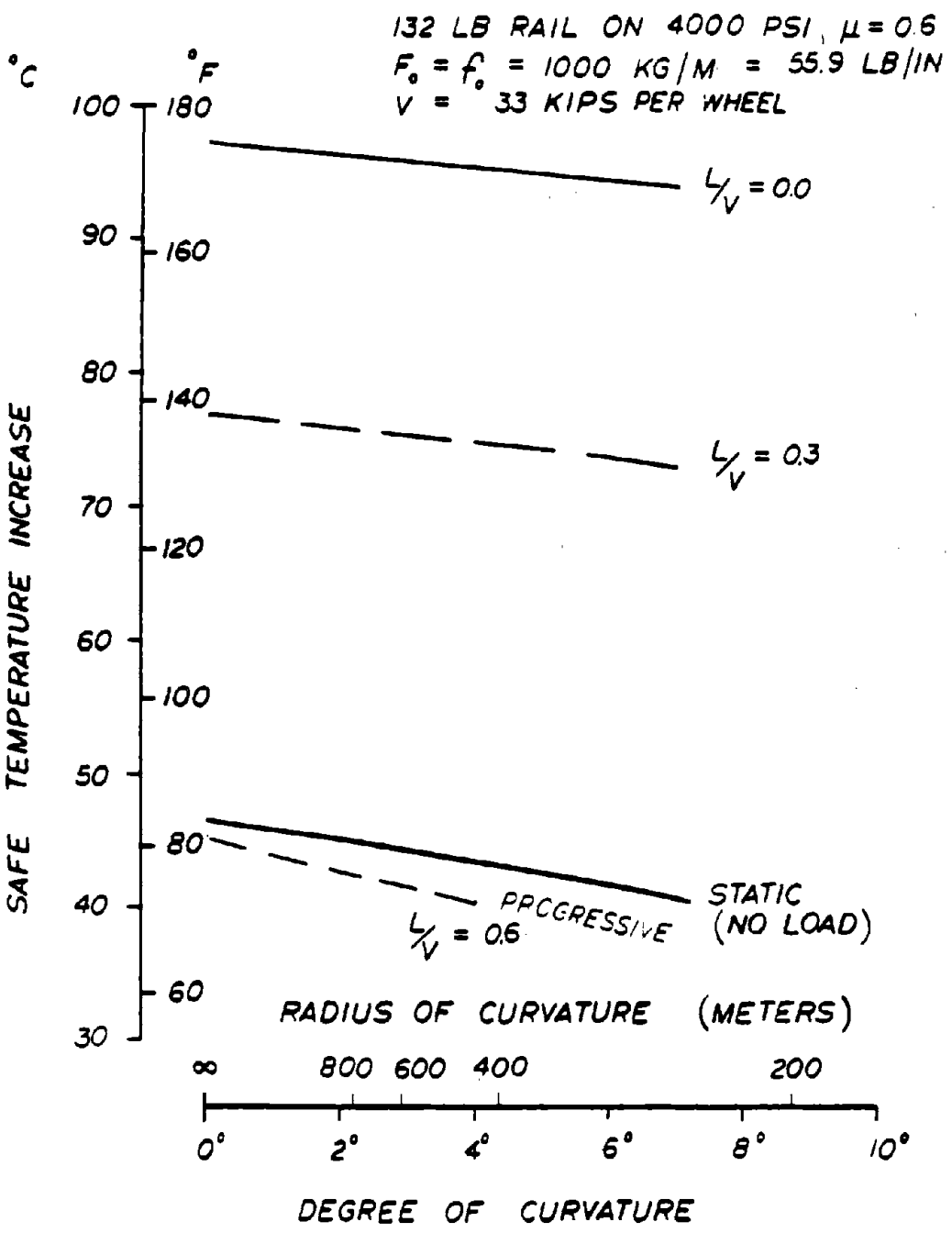

FIGURE 3.6 - EFFECT OF TRUCK LOADS ON SAFE TEMPERATURE INCREASE FOR CURVED TRACKS

not important for stability considerations. As discussed earlier, lateral forces may be critical in the generation of misalignments.

Regardless of the presence of lateral wheel loads, the effect of vertical vehicle loads can be to produce negative (upwards) bending deflection at some distance away from the wheels. The upward bending "wave" can reduce the lateral resistance. Of course, the lateral resistance elsewhere, particularly under the wheels, will increase. The net effect can be increased or reduced buckling strength of the track.

The bending wave for a GP38-2 locomotive and hopper car consist is shown in Figure 3.7. For the sake of appropriate terminology, the following zones are defined:

- o Precession Wave: This is the region of upward negative deflection in front of the locomotive. The deflection is due to bending of track in the vertical plane under the influence of wheel loads. The deflection is measured with respect to the equilibrium level of the track under self weight.

- o Central Wave: This is the region of upward negative deflection in the central region between the two trucks. The deflection is due to bending in the vertical plane under the influence of wheel loads and is measured with respect to the equilibrium level of the track due to self-weight.

- o Recession Wave: This is defined in the same way as the precession wave, except that it occurs behind the trailing car in the consist.

It must be remarked that the foregoing upward bending deflections do not necessarily result in the track lifting off the ballast bed. This is because of the self weight of the track inducing downward deflection which can be larger than the upward deflection due to bending. Whether or not the track actually lifts off the ballast bed, some loss of lateral

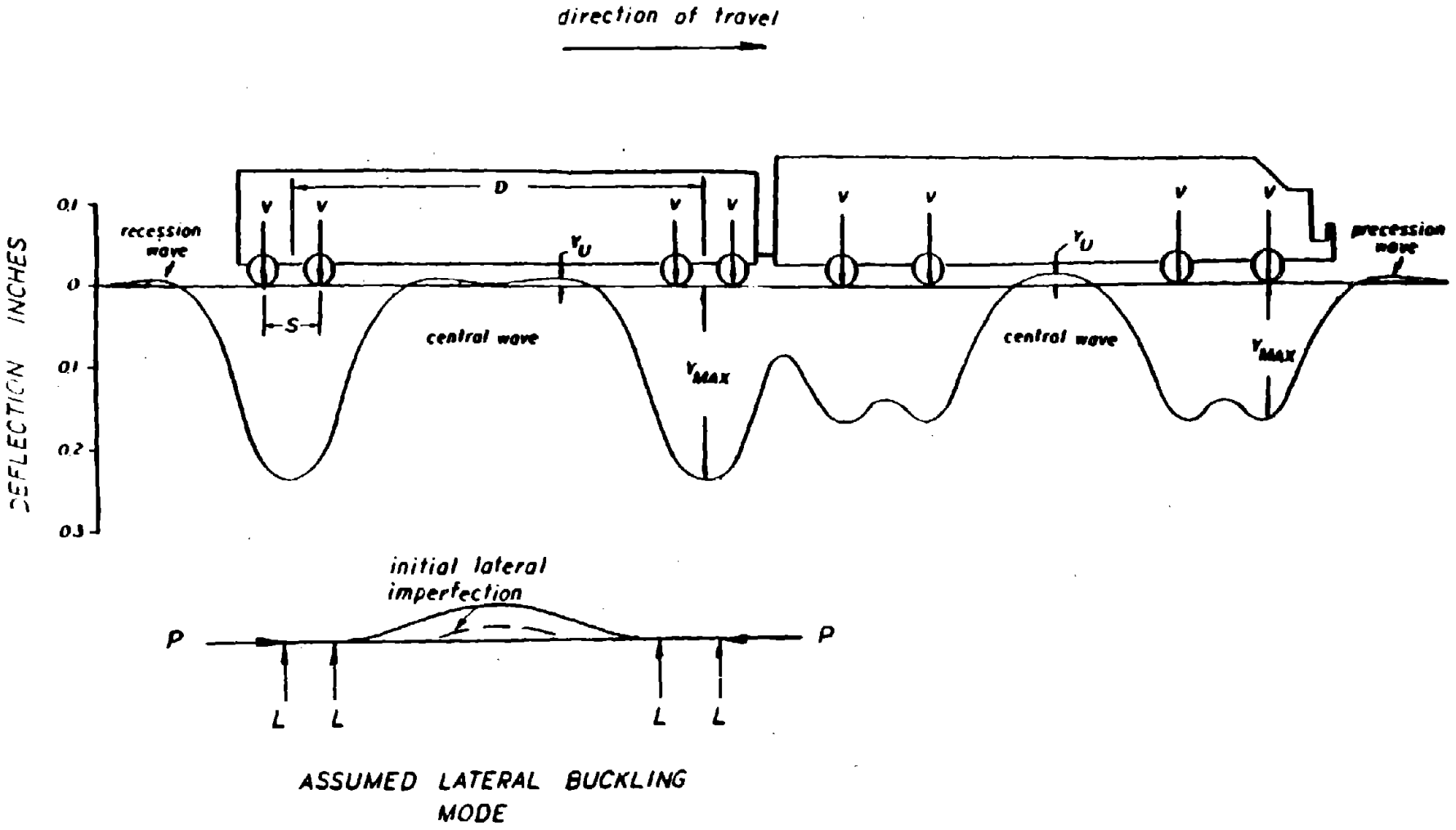

FIGURE 3.7 - TYPICAL TRACK DEFLECTIONS DUE TO GP38-2 LOCOMOTIVE AND HOPPER CAR

resistance in precession, central and recession "waves" will take place.

Basically, the upward bending wave reduces reaction between ties and ballast, and hence reduces the lateral resistance. The latter equals the product of the reaction and the tie-ballast friction plus the resistance due to ballast shoulder and side friction.

To determine the net reaction between ballast and ties, the "standard analysis" is used which is a superposition of solutions of the Winkler foundation model and the self weight. If there is any track lift-off, the reaction between ballast and tie is taken as zero in the lift-off region. Consequently, in the lift-off region there are only two components contributing to the lateral resistance (i.e., shoulder and side friction), which are taken independent of the amount of lift (see Appendix A).

In the course of this work, a "tensionless" foundation model as discussed by Kerr has been examined [16]. This is more rigorous than the standard analysis, since this model does not assume the ballast to be in tension in the lift-off zone. Calculations have shown, however, that the two models do not yield significantly different results for the lift-off zone, though the amplitudes of lift-off in the models could differ. Since the lateral resistance in the lift-off zone is assumed to be independent of the amount of lift-off, the standard analysis employed here can be expected to be of sufficient accuracy.

Another assumption implied in the present analysis is that the rails are rigidly attached to the ties by the fasteners; therefore, the vertical deflections of rails and ties will be the same. There are many rail fasteners which satisfy this rigid connection assumption. In cut-spike construction for wood ties, the rigid condition is achieved only when spikes are tight and fully driven. This situation is not uncommon and buckling assessments made on such a basis may be conservative. In general, there is some finite clearance between spike heads and the rail base, which will permit some initial vertical movement of rails before they tend to lift up the ties. It is convenient to consider the following scenarios that may exist in typical tracks:

- o Zero Clearance: Rigid connection between rails and ties is implied as stated earlier. This typically occurs in new track after rail replacement. The central bending wave in between trucks will reduce the vertical pressure between tie bottom and the ballast causing reduced lateral resistance as described in this work.

- o "Large" Clearance (greater than 1/4 inch): This can arise if spikes are loose. The central bending wave due to truck loads will deflect the rails upwards without carrying ties. Therefore, the lateral resistance reduces only slightly due to rail lift-off. Using tensionless foundation models, calculations have been carried out in References 16 and 21 for the rail lift-off in the case of precession bending wave. For a single truck with wheel loads of the order of 33 kips the rail lift-off is found to be of the order of 1/4 inch. Calculations have not been performed for the central bending wave due to the two trucks, but rail lift-off is expected to be larger than 1/4 inch. In the presence of rail thermal (compressive) forces, this value will further increase.

- o "Small" Clearance (less than 1/8 inch): The average clearance between spike heads and rail base in typical tracks is generally considered to be of the order of 1/8 inch. From the foregoing discussion of rail lift-off in the case of large clearance, it is clear that due to vehicle vertical loads, the rails tend to lift up the ties or reduce the normal pressure between ties and ballast, if the clearance is less than 1/4 inch. An improved tensionless foundation model that accounts for finite clearance (on the order of 1/8 inch) and central bending wave under truck loads will be presented in a forthcoming publication [14]. This model will simultaneously account for the increased lift due to temperature increase and consequent reduction in the lateral resistance. It is anticipated, however, that the improved theory will yield dynamic buckling strength values of the same order as the simplified theory presented here.

Referring to Figure 3.7, the symmetric mode in between the trucks of a vehicle is considered critical because of central wave uplift. Buckling potential exists also in the front or rear of a consist due to precession/recession waves. This will be examined later.

In this section, the safe and buckling temperature increases under the influence of the central wave produced by various vehicles are determined. The effect of lateral imperfections and vertical track stiffness will also be examined.

The vehicles considered in these analyses are listed in Table 2 in ascending order of truck center spacing, D (see Figure 3.7). The Ore Car has the smallest value whereas the Wood Chip car has the largest value for the truck center spacing. The axle spacing and the wheel loads for the vehicles are also shown in the table.

Vertical deflection profiles due to wheel loads (self weight not included) are presented in Figures 3.8 and 3.13. All vehicles with the exception of the Ore Car (Figure 3.8) have exhibited central wave (vertical upward deflection in the central zone) for the assumed wheel loads. The vertical foundation modulus is assumed to be fixed at 4000 psi for the track (two rails considered) unless otherwise stated.

The positive downward deflection under the Ore Car, resulting in higher deflection will tend to increase the lateral buckling strength of the track.

For all other vehicles considered a central bending wave exists under the vehicle in between the trucks, therefore, lateral buckling can take place under the car due to the reduction in the lateral resistance.

The length of central wave varies from 6 feet for the GP38-2 Locomotive to about 24 feet for the Wood Chip Car (In Figure 3.13, there are actually two central waves). Track uplift deflections are typically on the order of 0.01 inches.

3.3.1 Safe Temperature Increases

Figure 3.14 shows the values of safe temperature increase for tangent track with lateral resistances of 55.9 lb/in (1000 kg/m) and 33.5 lb/in (600 kg/m). The truck center spacing of the vehicles is taken as the independent variable and is shown as such on the x-axis (abscissa). The track modulus, k_v, is taken as 4000 psi (per two rails) and other parameters assumed are shown in Figure 3.14. The safe temperature increase values decrease with increasing truck center spacing and approach the values for track without vehicles, which are denoted as

TABLE 2 - VEHICLE PARAMETERS

VEHICLE	TRUCK CENTER SPACING inches (meters) [D]	AXLE SPACING inches (meters) [S]	WHEEL LOAD pounds (kilograms) [V]
Ore car	182. (4.6228)	60. (1.5240)	24338. (11040.)
GP38-2 Locomotive	408. (10.3632)	108. (2.7432)	31250. (14175.)
U28B Locomotive	434. (11.0236)	112. (2.8448)	33750. (15309.)
Covered Hopper Car	506. (12.8524)	70. (1.7780)	32875. (14912.)
Large Tank Car	616.125 (15.6496)	99. (2.5146)	39375. (17860.)
Wood Chip Car	619. (15.7226)	70. (1,7780)	32925. (14935.)

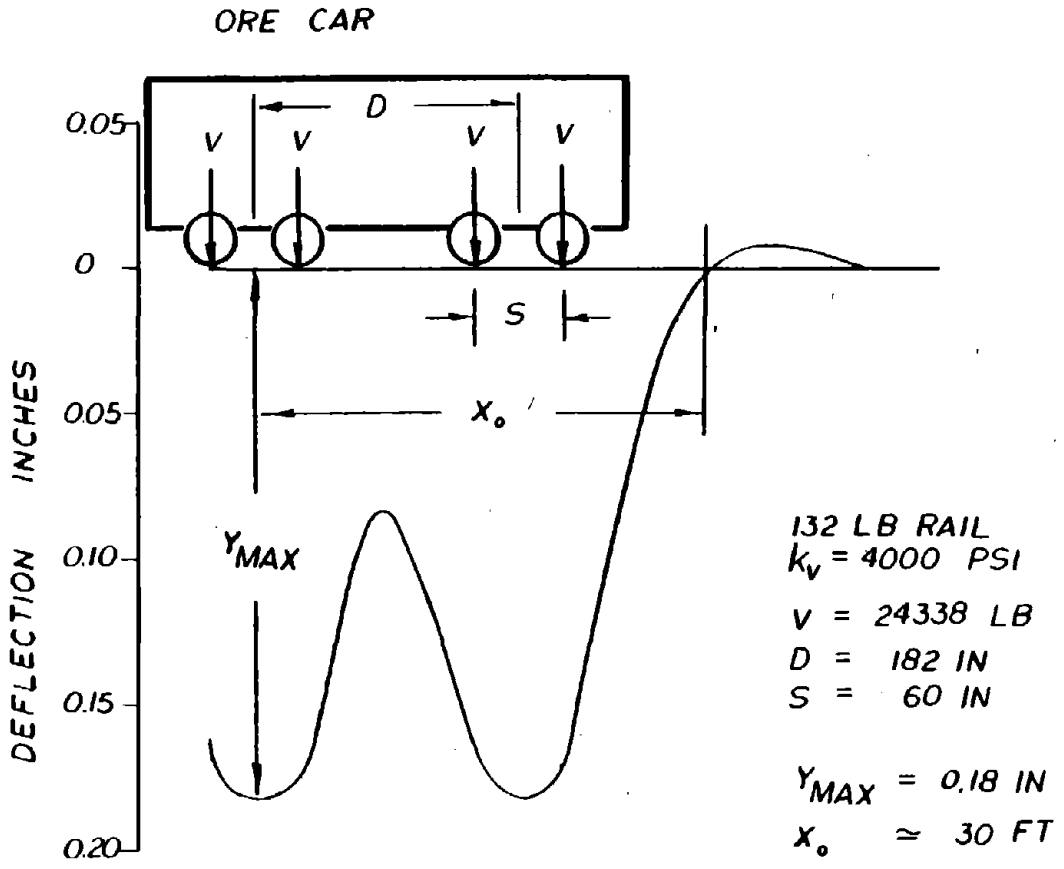

FIGURE 3.8 - VERTICAL DEFLECTION OF TRACK UNDER ORE CAR

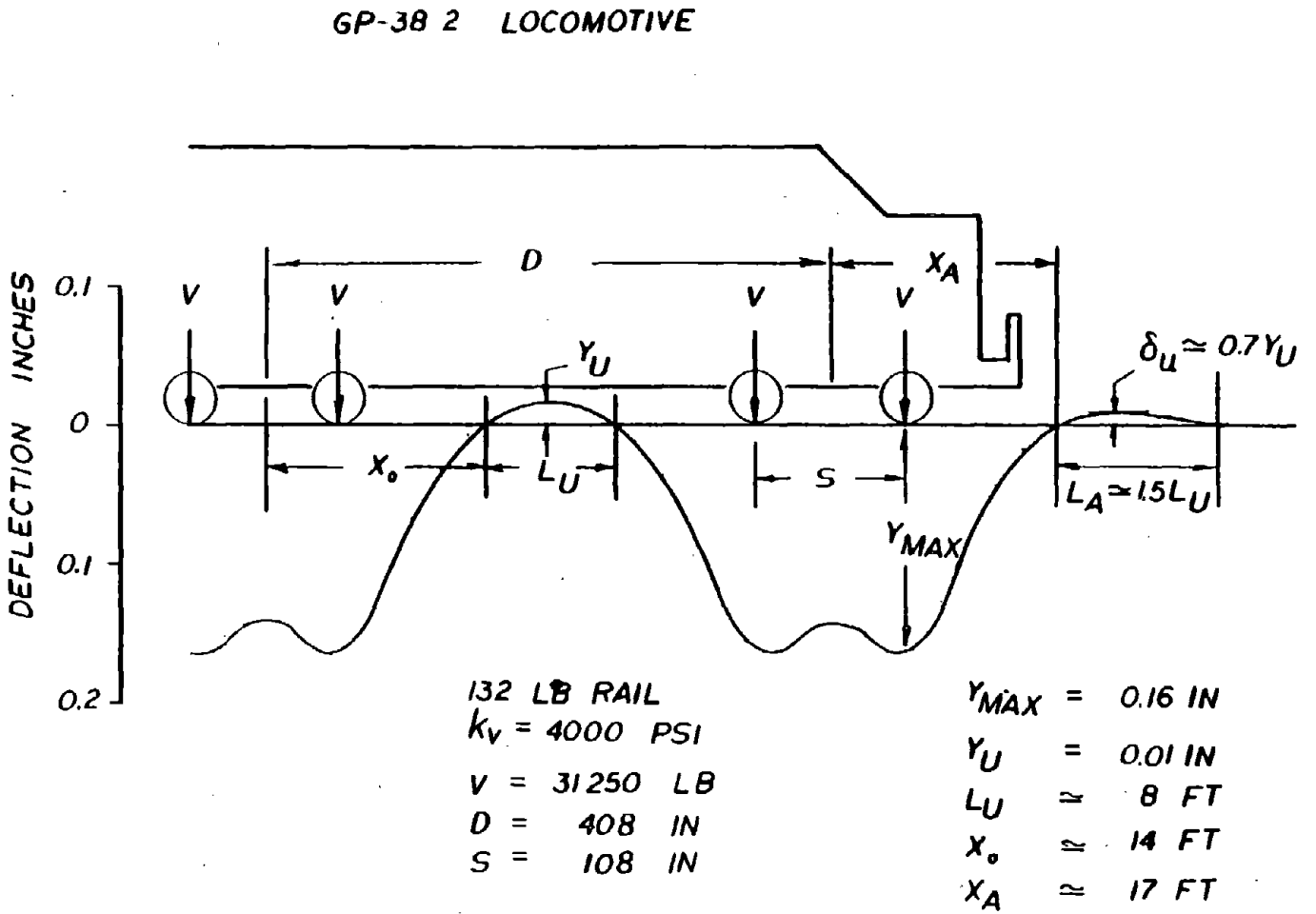

FIGURE 3.9 - VERTICAL DEFLECTION OF TRACK UNDER GP38-2 LOCOMOTIVE

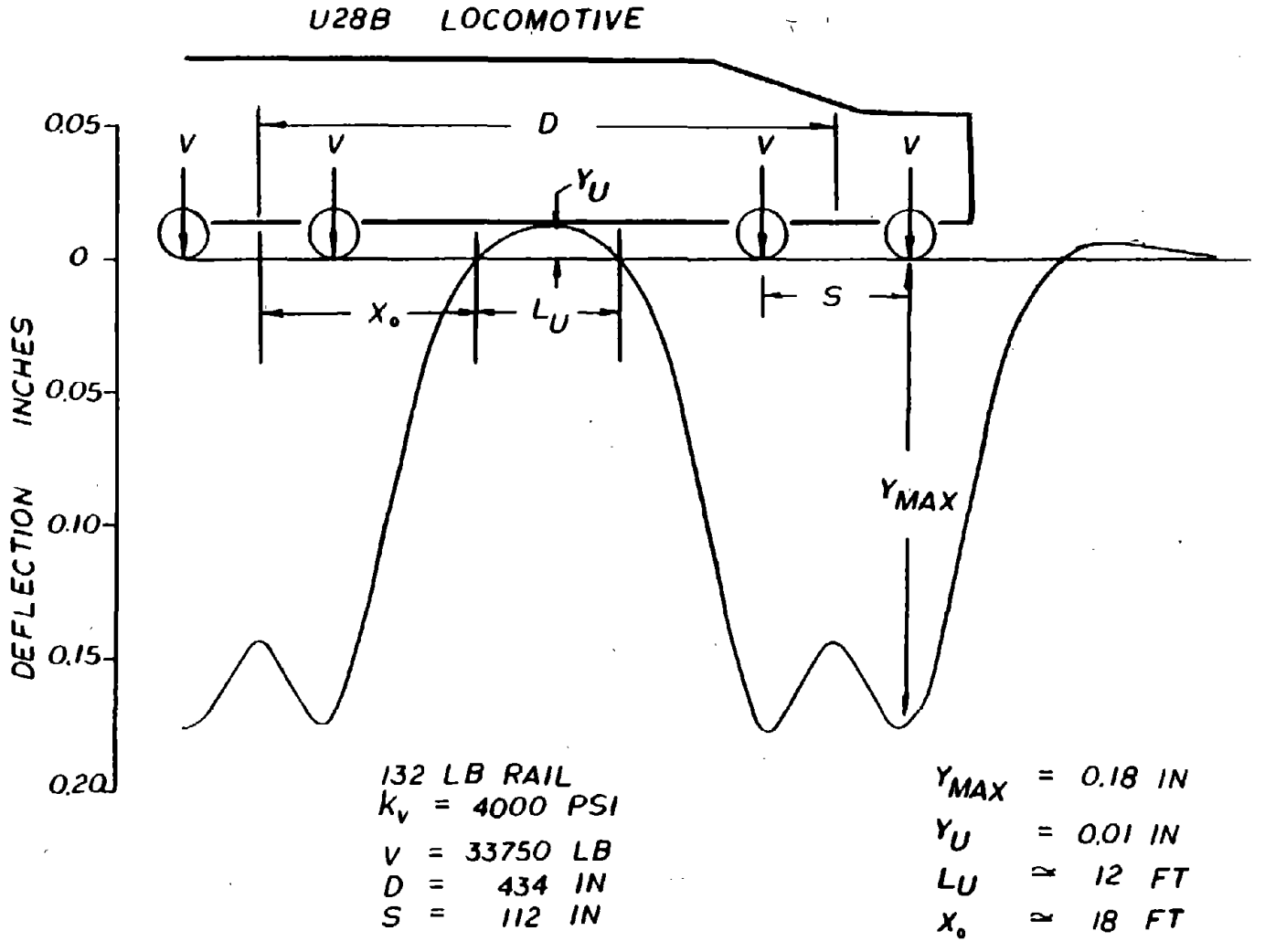

FIGURE 3.10 - VERTICAL DEFLECTION OF TRACK UNDER U28B LOCOMOTIVE

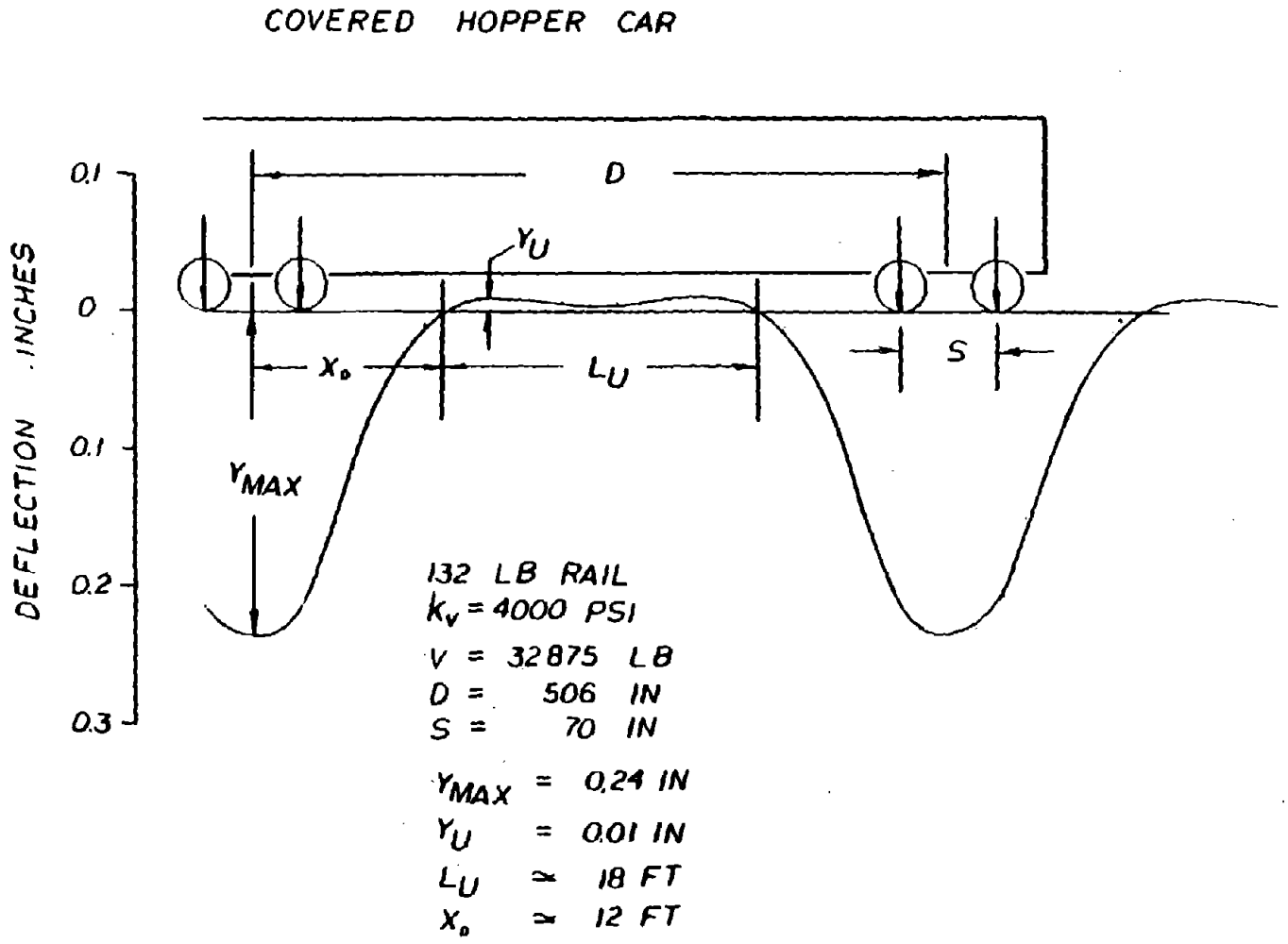

FIGURE 3.11 - VERTICAL DEFLECTION OF TRACK UNDER COVERED HOPPER CAR

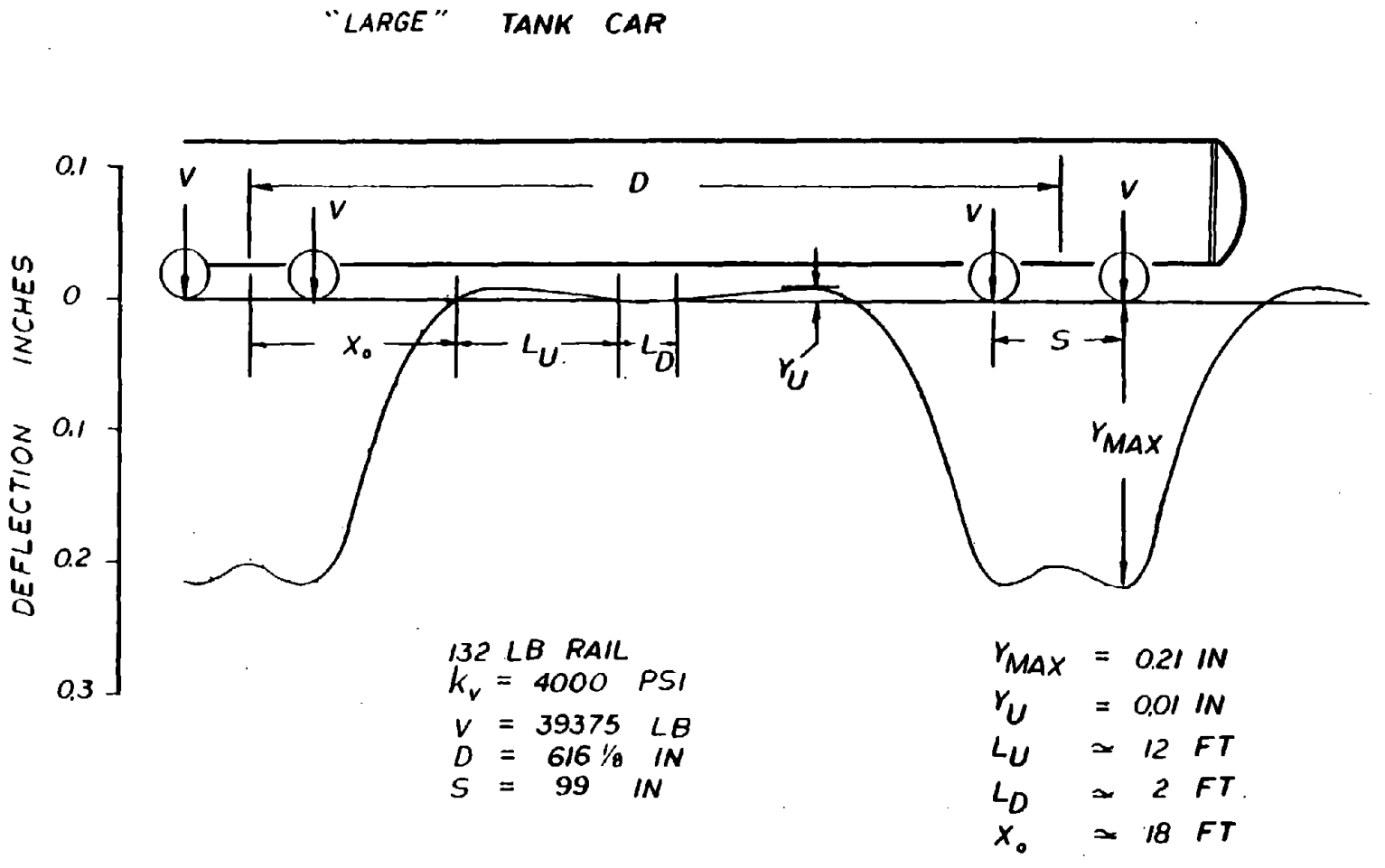

FIGURE 3.12 - VERTICAL DEFLECTION OF TRACK UNDER MONSANTO TANK CAR

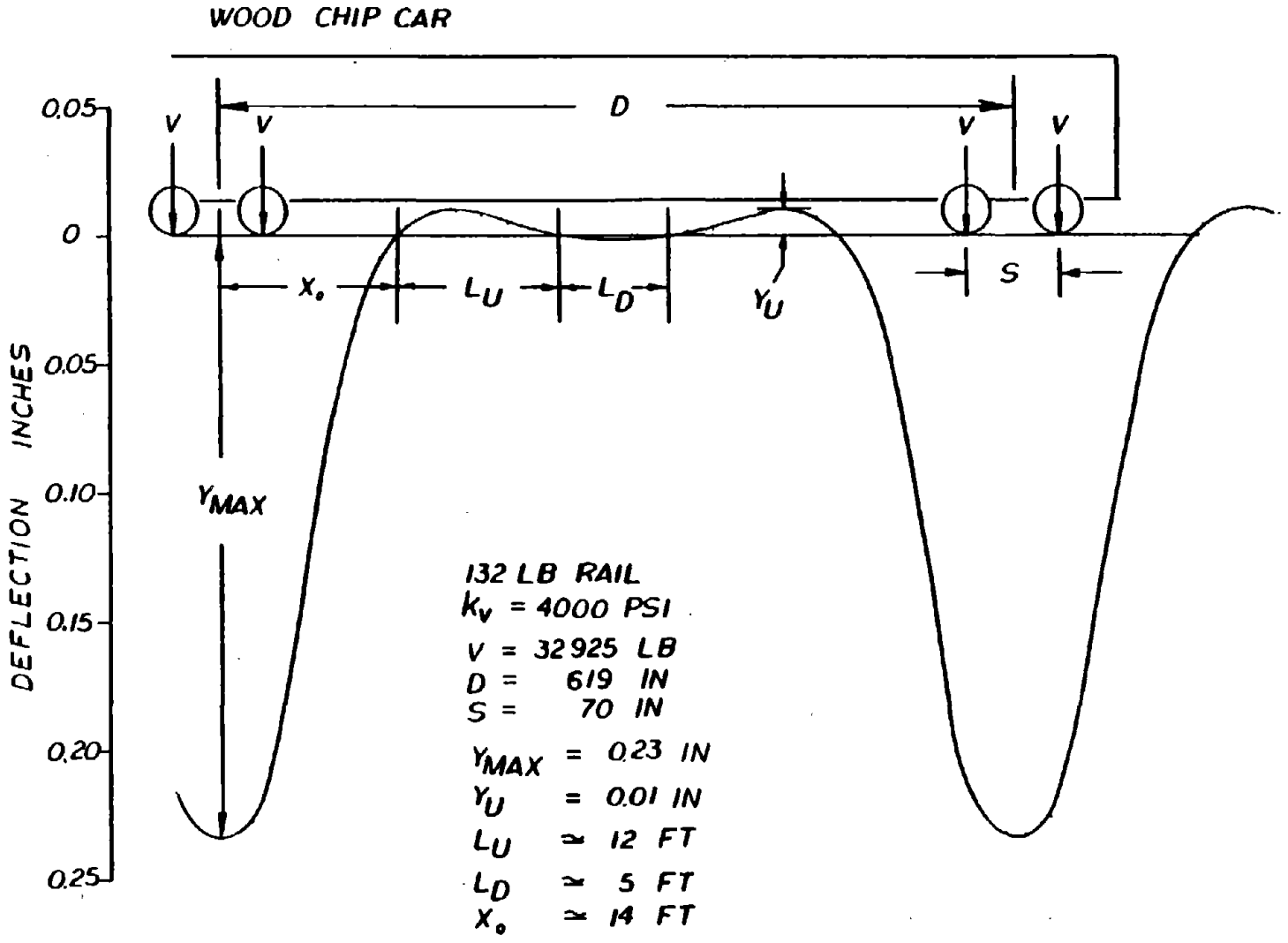

FIGURE 3.13 - VERTICAL DEFLECTION OF TRACK UNDER WOOD CHIP CAR

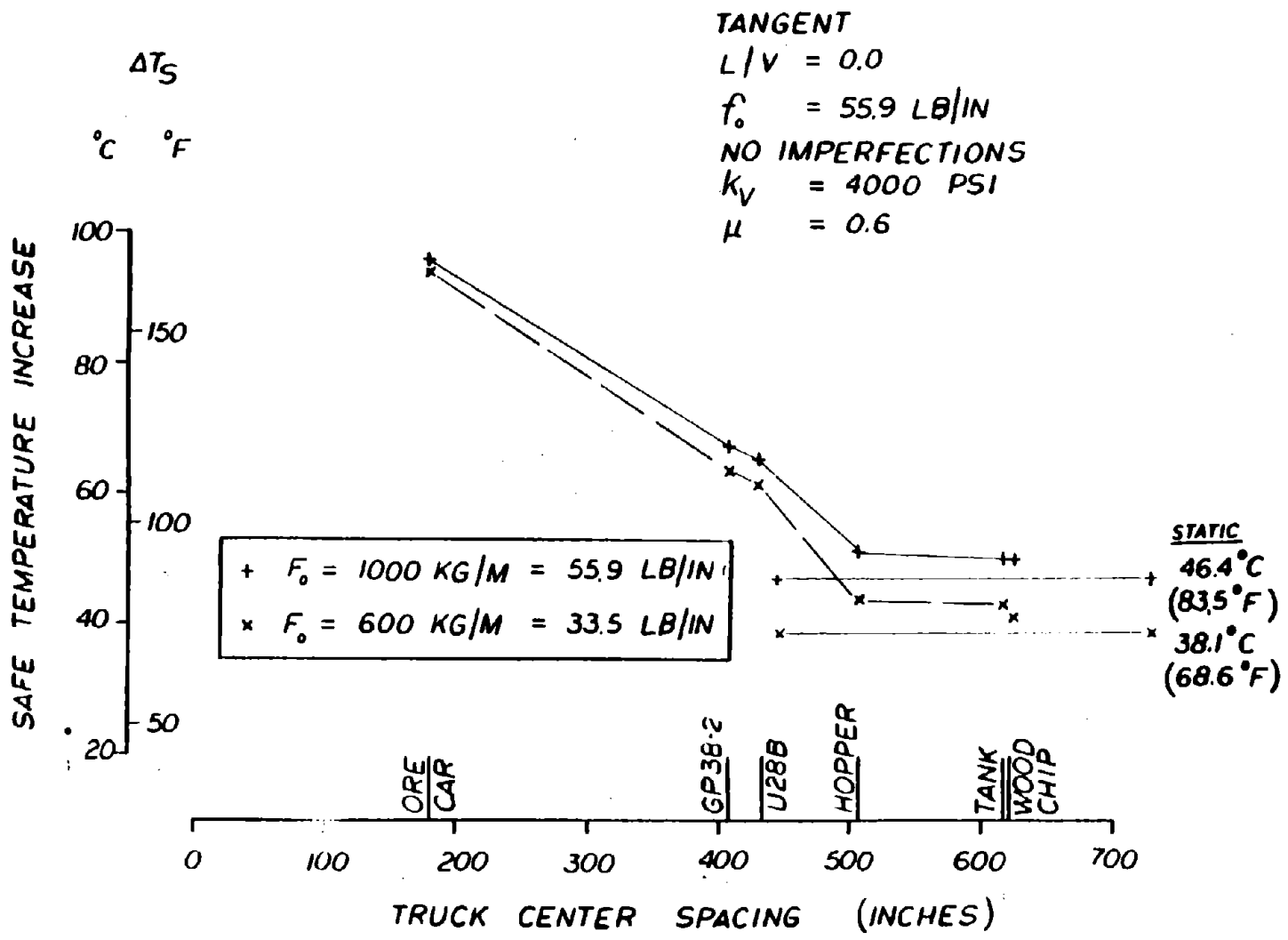

FIGURE 3.14 – EFFECT OF TRUCK CENTER SPACING ON SAFE TEMPERATURE INCREASE (VARYING LATERAL RESISTANCE)

theoretical "static" values.

The safe temperature increases for 5^{o} curved track under vehicle loads are shown in Figures 3.15 for F_o = 33.5 lb/in (600 kg/m) and in Figure 3.16 for F_o = 55.9 lb/in (1000 kg/m). Again, for the Tank and the Wood Chip Car (i.e., cars with large truck center spacing) the safe temperature increase values approach the "static" values. It can be shown that for L/V = 0.6 and F_o = 33.5 lb/in (600 kg/m) "progressive buckling" occurs, i.e. there is no distinct safe temperature increase value and, therefore, results for L/V = 0.6 are not shown in Figures 3.15 and 3.16. From the results shown in these figures it can be concluded that for L/V ratios less than the friction coefficient, μ, short car influence results in a higher lateral buckling strength, whereas, long car influences are practically unaffected by L/V ratio, as one would expect.

3.3.2 Effect of Imperfections: Buckling Temperature Increases

When a symmetric lateral imperfection is present (as in Figure 3.7) in the track, buckling can occur between the trucks. The effect of imperfections under various scenarios is presented in Figures 3.17 to 3.24.

Figures 3.17 to 3.19 show the results for the GP38-2 Locomotive on tangent and curved tracks with imperfections. These results show that the dynamic safe temperature increases are higher than the static values; the dynamic buckling temperatures, ΔT_B, are also generally higher than the static ΔT_B depending on imperfection size and track curvature. Thus a GP38-2 locomotive has, in general, a stabilizing effect on the track as far as buckling between the trucks is concerned.

The results for the Covered Hopper Car are shown in Figures 3.20 to 3.22. It is clear from these figures that the buckling temperature increases are generally reduced due to the presence of a vehicle but the safe temperature increases are not appreciably influenced. This is in contrast with the conclusion reached for the GP38-2 locomotive for which the safe temperature increases are significantly higher and the buckling temperature increases can also be higher than the static values.

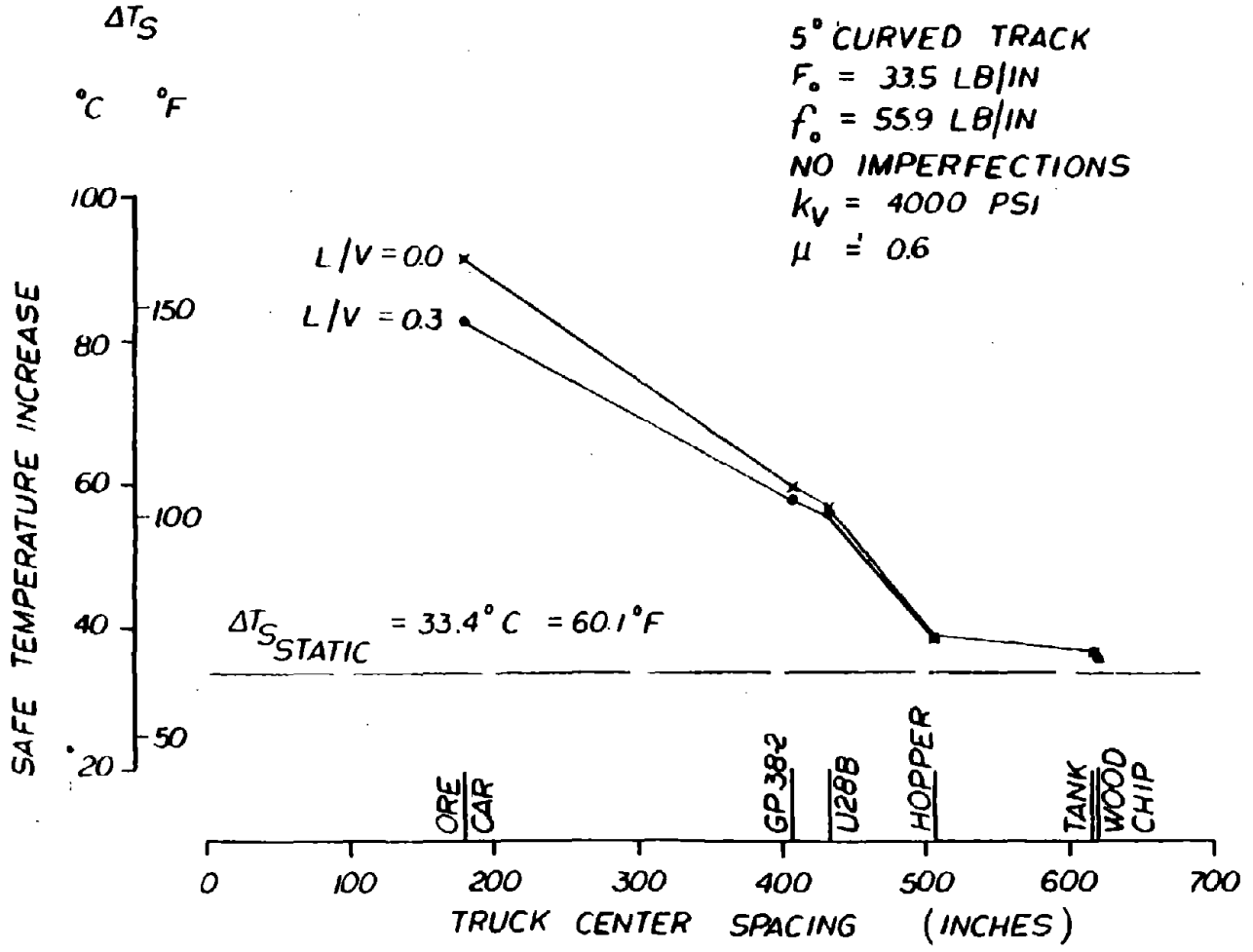

FIGURE 3.15 - EFFECT OF TRUCK CENTER SPACING ON SAFE TEMPERATURE INCREASE FOR 5° CURVED TRACK (VARYING L/V RATIO)

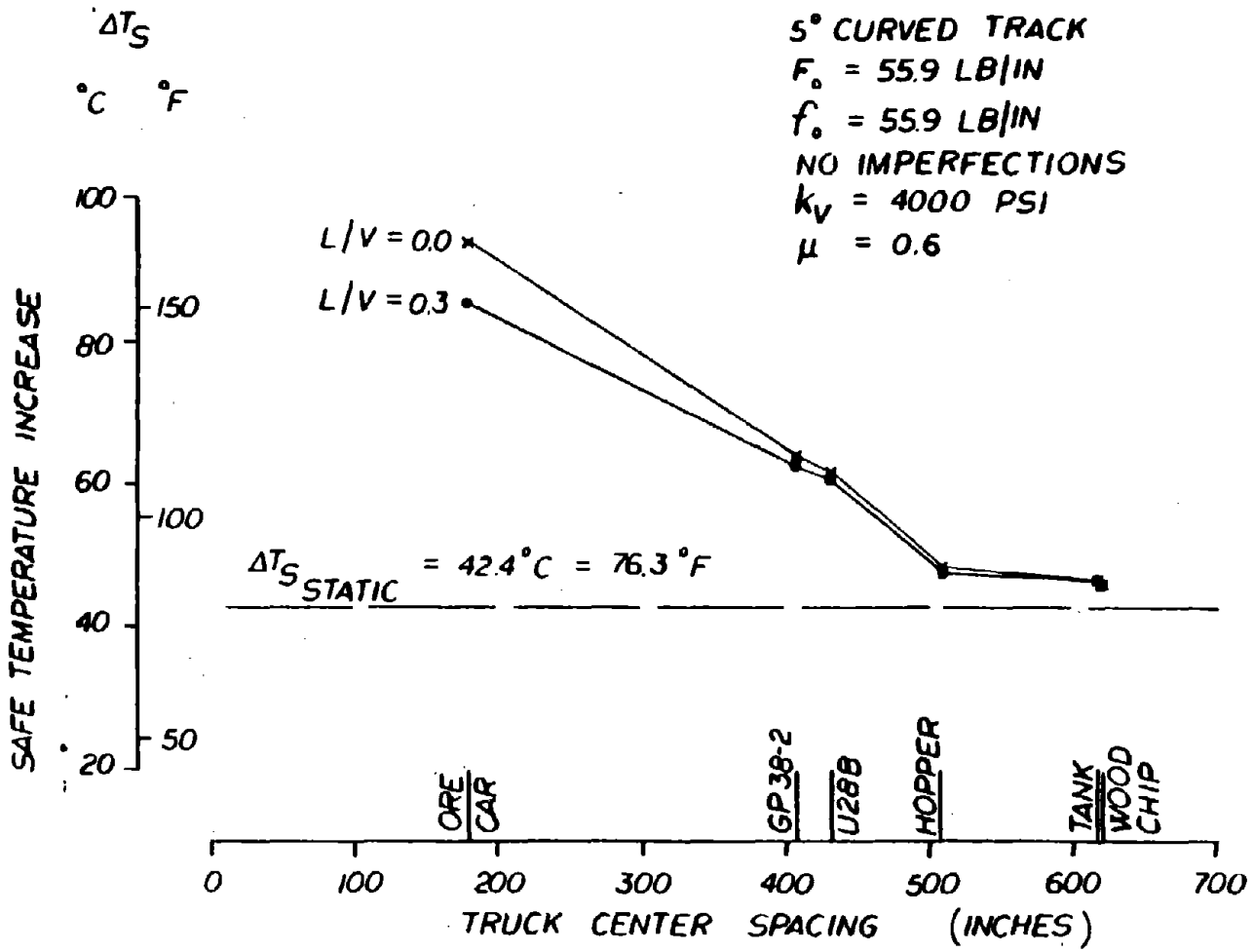

FIGURE 3.16 - EFFECT OF TRUCK CENTER SPACING ON SAFE TEMPERATURE INCREASE

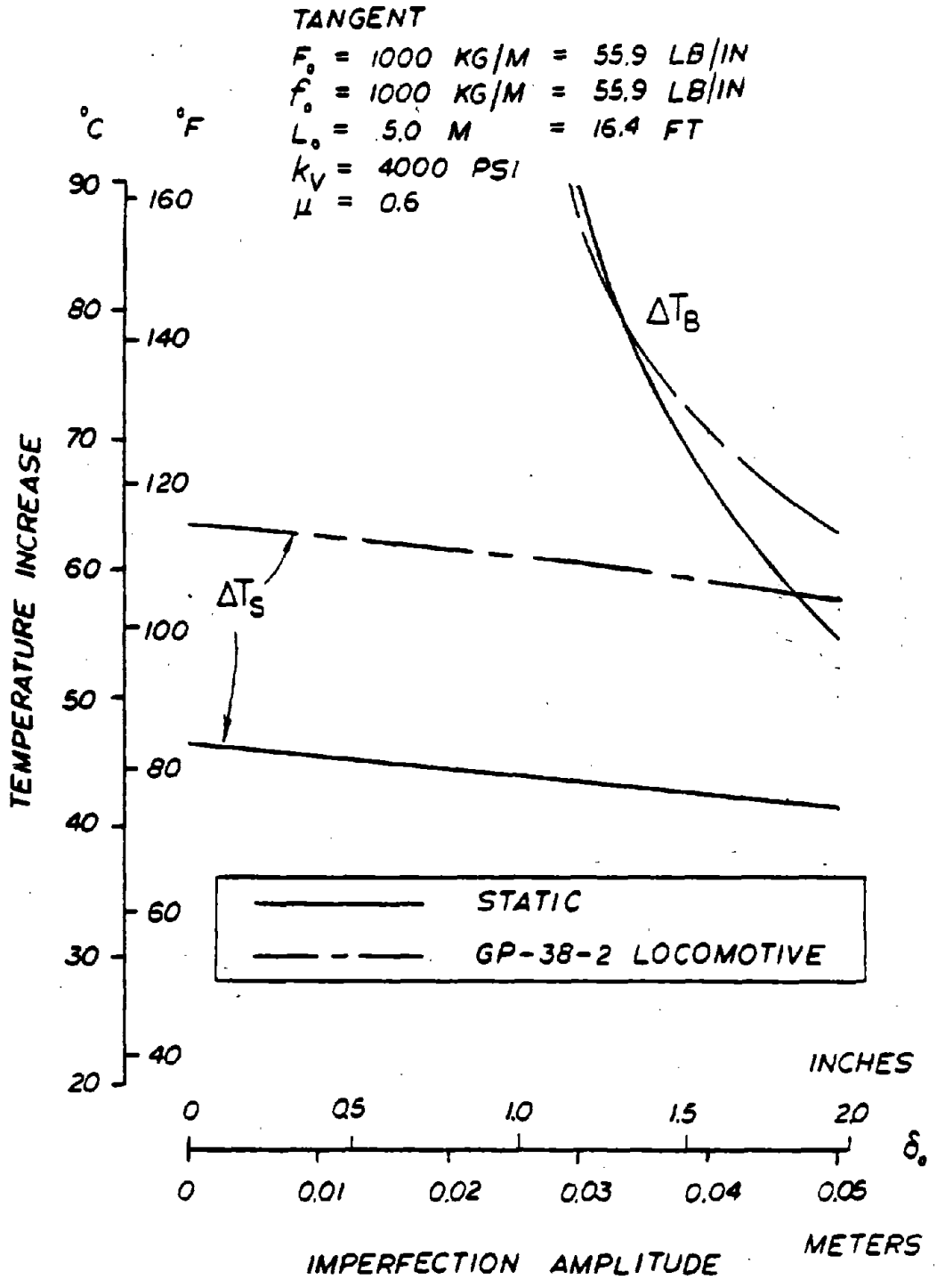

FIGURE 3.17 - EFFECT OF IMPERFECTION AMPLITUDE ON SAFE TEMPERATURE INCREASE AND BUCKLING TEMPERATURE INCREASE FOR STATIC VERSUS DYNAMIC (GP38-2 LOCOMOTIVE, TANGENT TRACK)

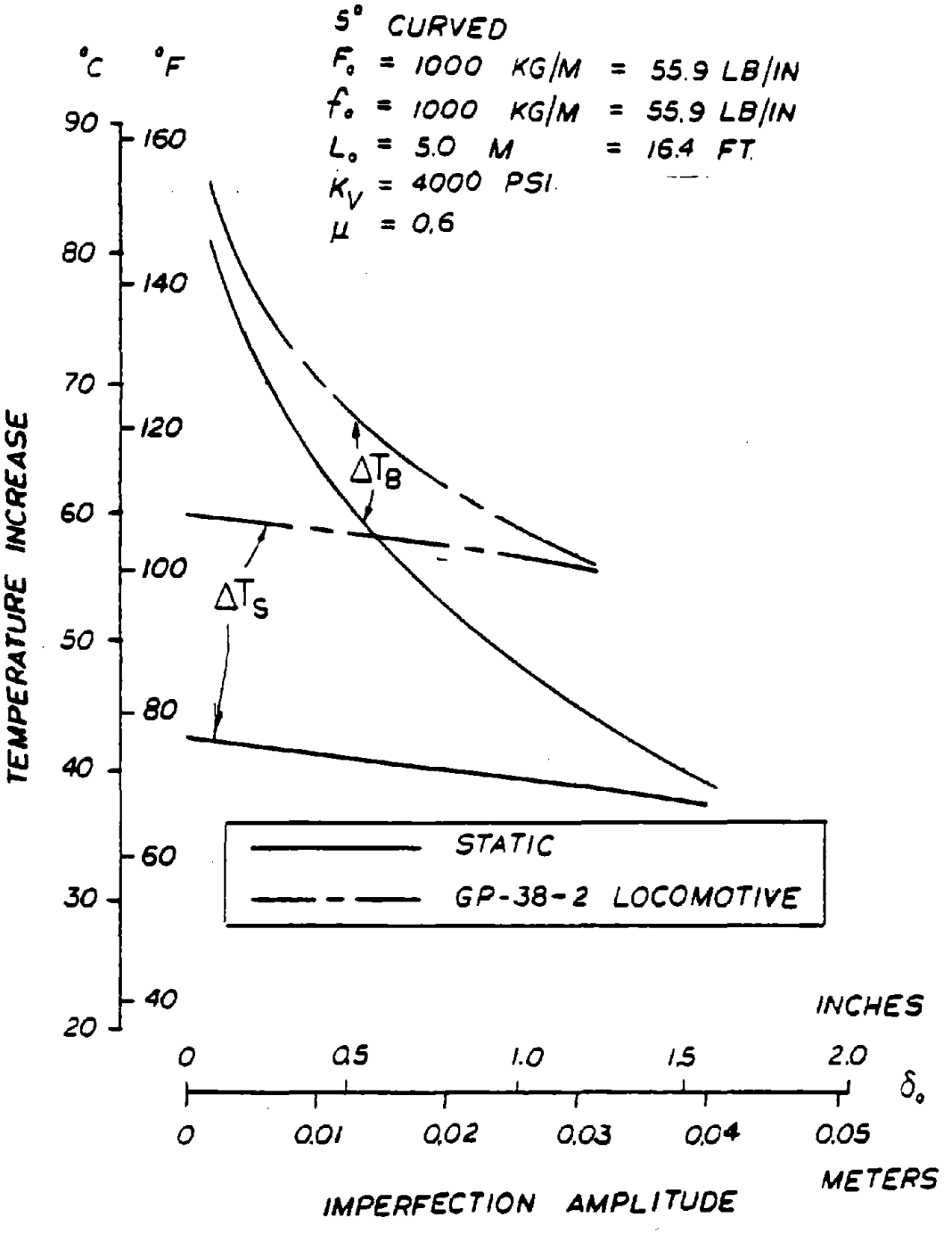

FIGURE 3.18 - EFFECT OF IMPERFECTION AMPLITUDE ON SAFE TEMPERATURE INCREASE AND BUCKLING TEMPERATURE INCREASE FOR STATIC VERSUS DYNAMIC (GP38-2 LOCOMOTIVE, 5° CURVED TRACK)

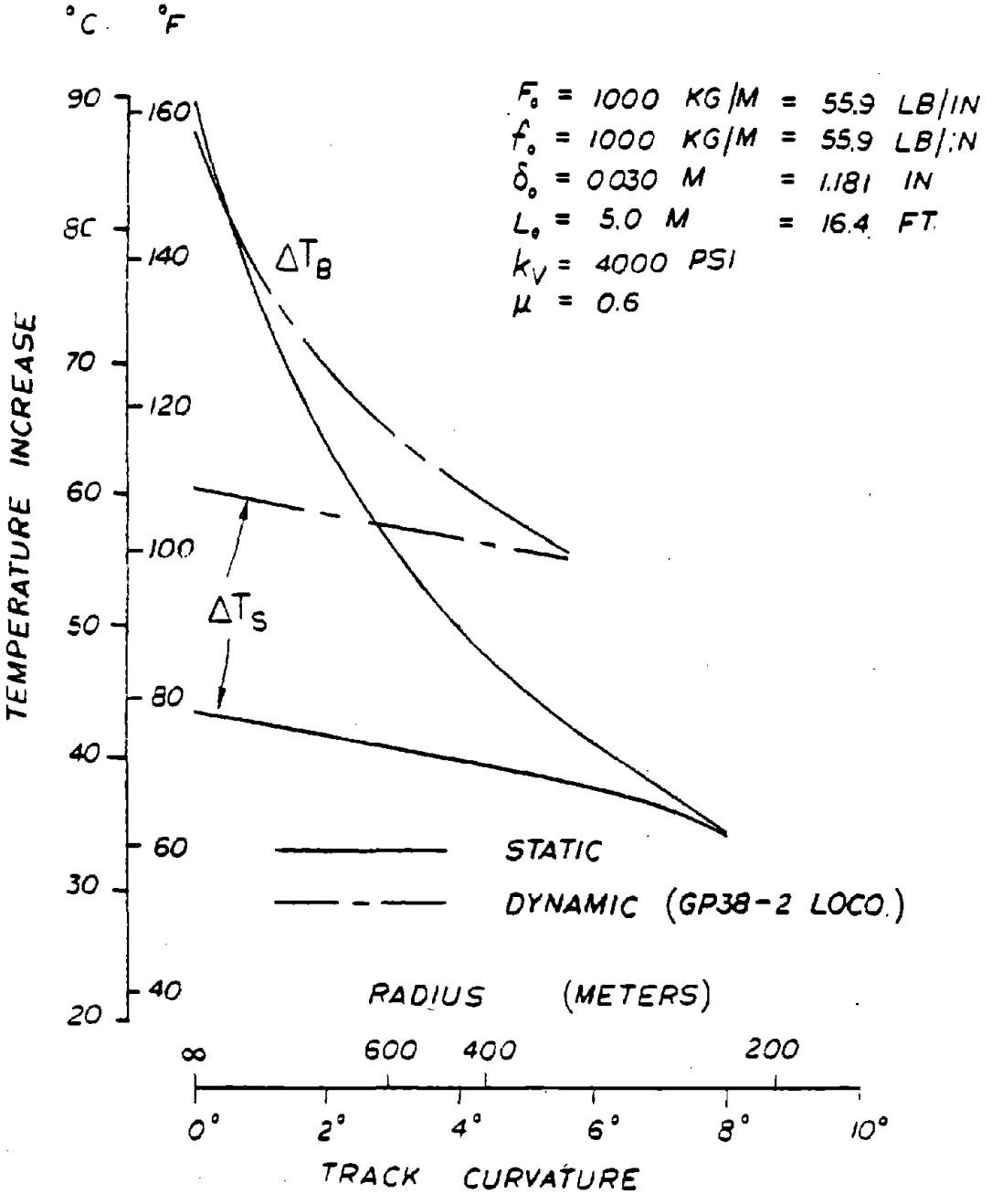

FIGURE 3.19 - STATIC VERSUS DYNAMIC (GP38-2 LOCOMOTIVE) INFLUENCE ON SAFE TEMPERATURE INCREASE AND BUCKLING TEMPERATURE INCREASE FOR CURVED TRACKS

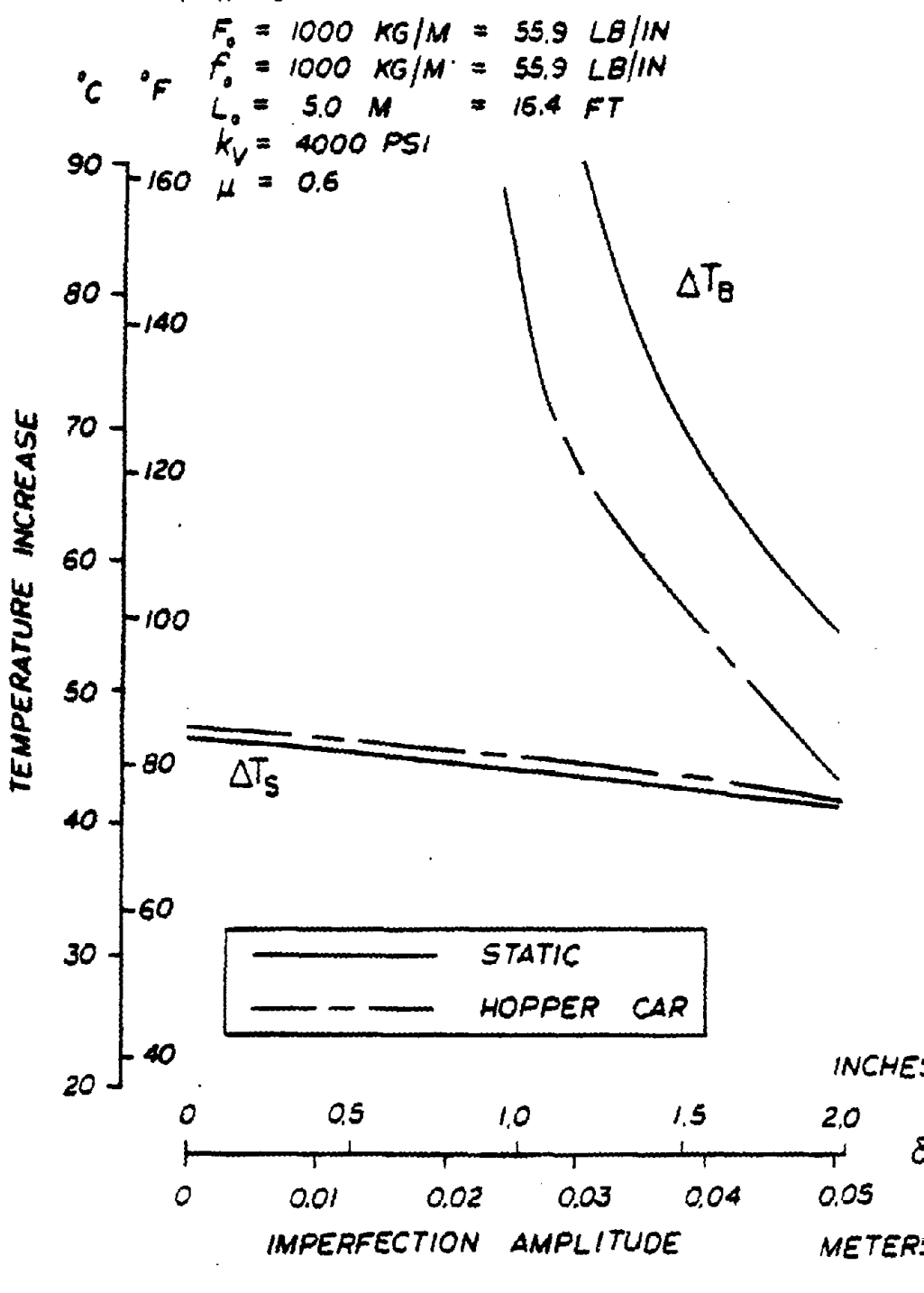

FIGURE 3.20 - EFFECT OF IMPERFECTION AMPLITUDE ON SAFE TEMPERATURE INCREASE AND BUCKLING TEMPERATURE INCREASE FOR STATIC VERSUS DYNAMIC (COVERED HOPPER CAR, TANGENT TRACK)

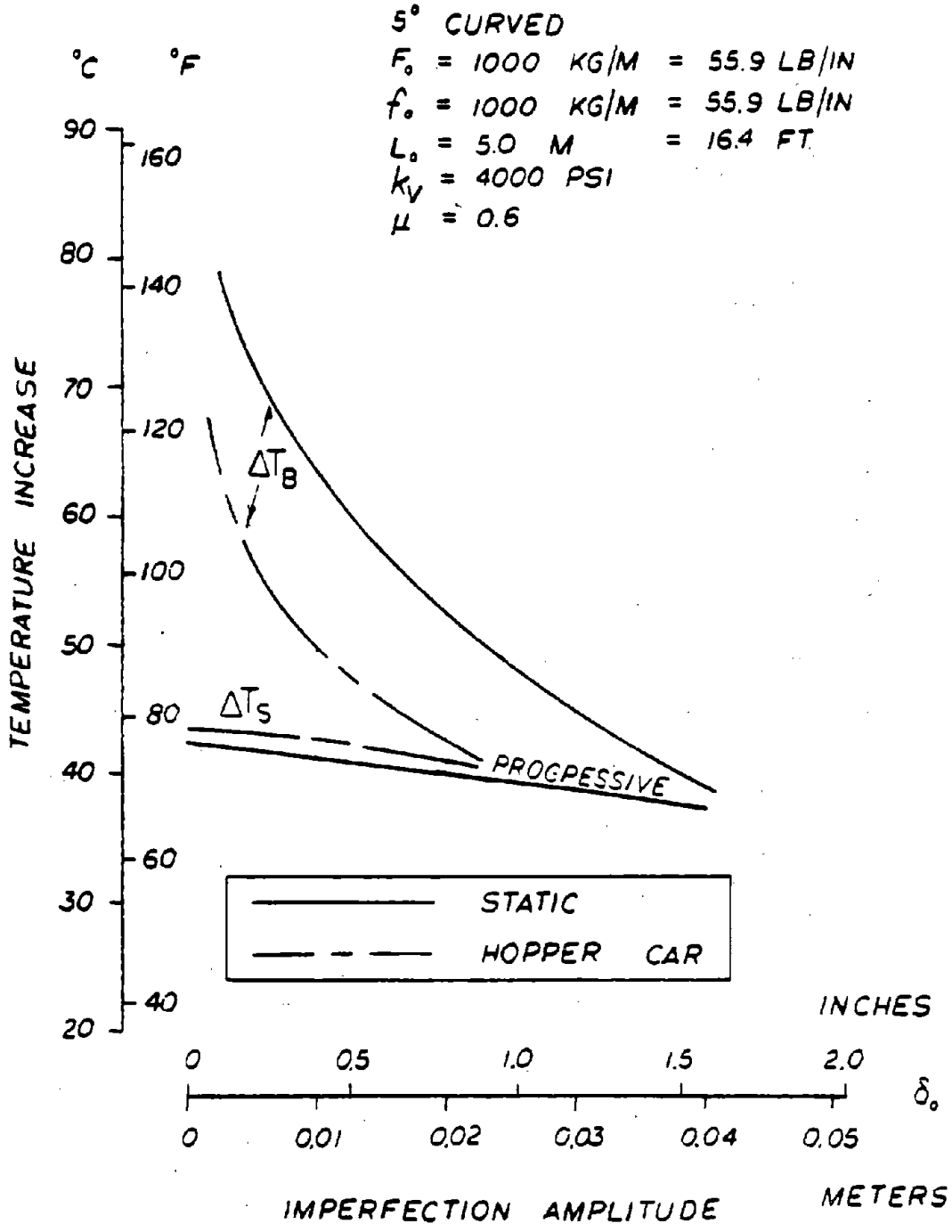

FIGURE 3.21 - EFFECT OF IMPERFECTION AMPLITUDE ON SAFE TEMPERATURE INCREASE AND BUCKLING TEMPERATURE INCREASE FOR STATIC VERSUS DYNAMIC (COVERED HOPPER CAR, 5° CURVED TRACK)

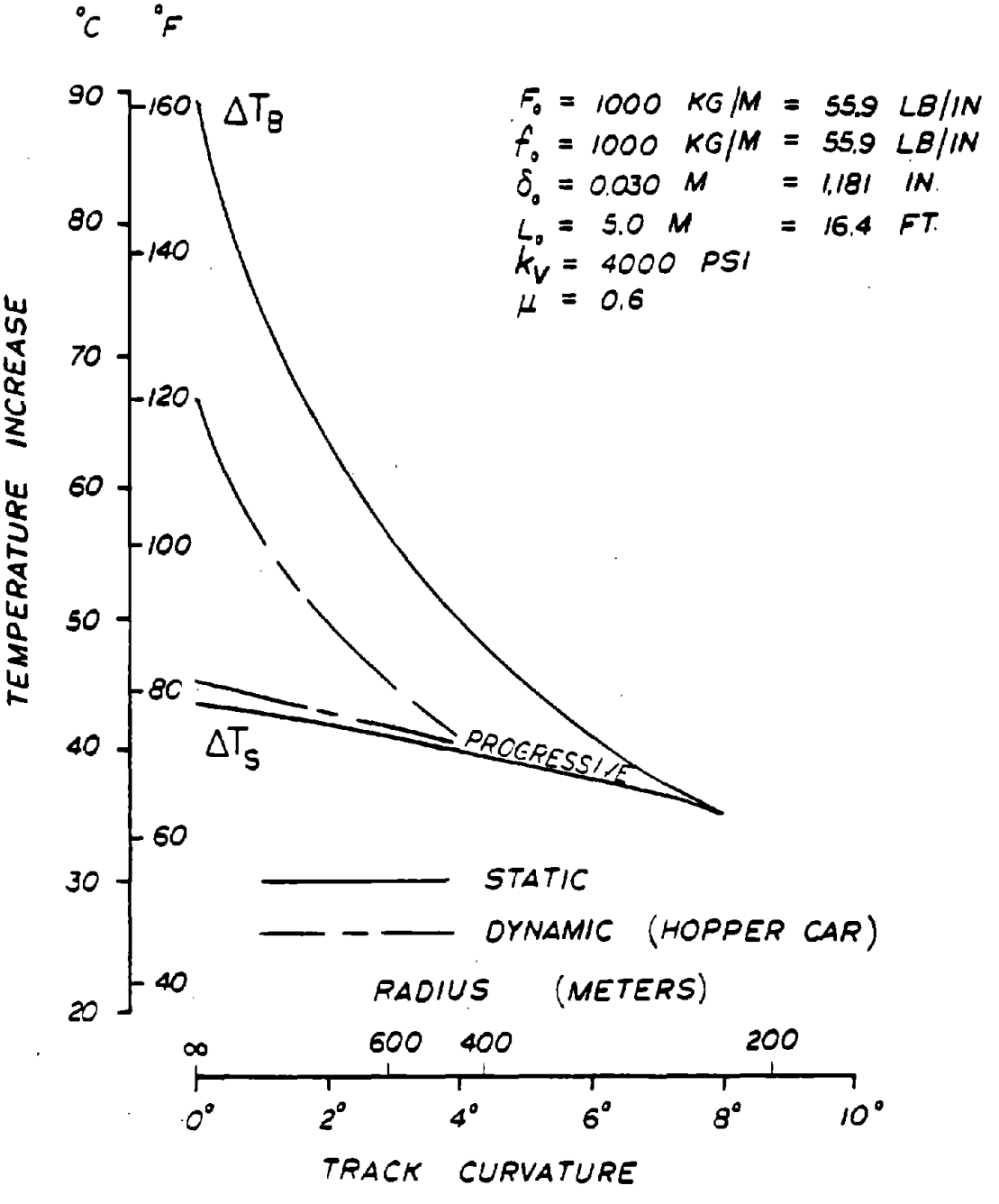

FIGURE 3.22 - STATIC VERSUS DYNAMIC (COVERED HOPPER CAR) INFLUENCE ON SAFE TEMPERATURE INCREASE AND BUCKLING TEMPERATURE INCREASE FOR CURVED TRACKS

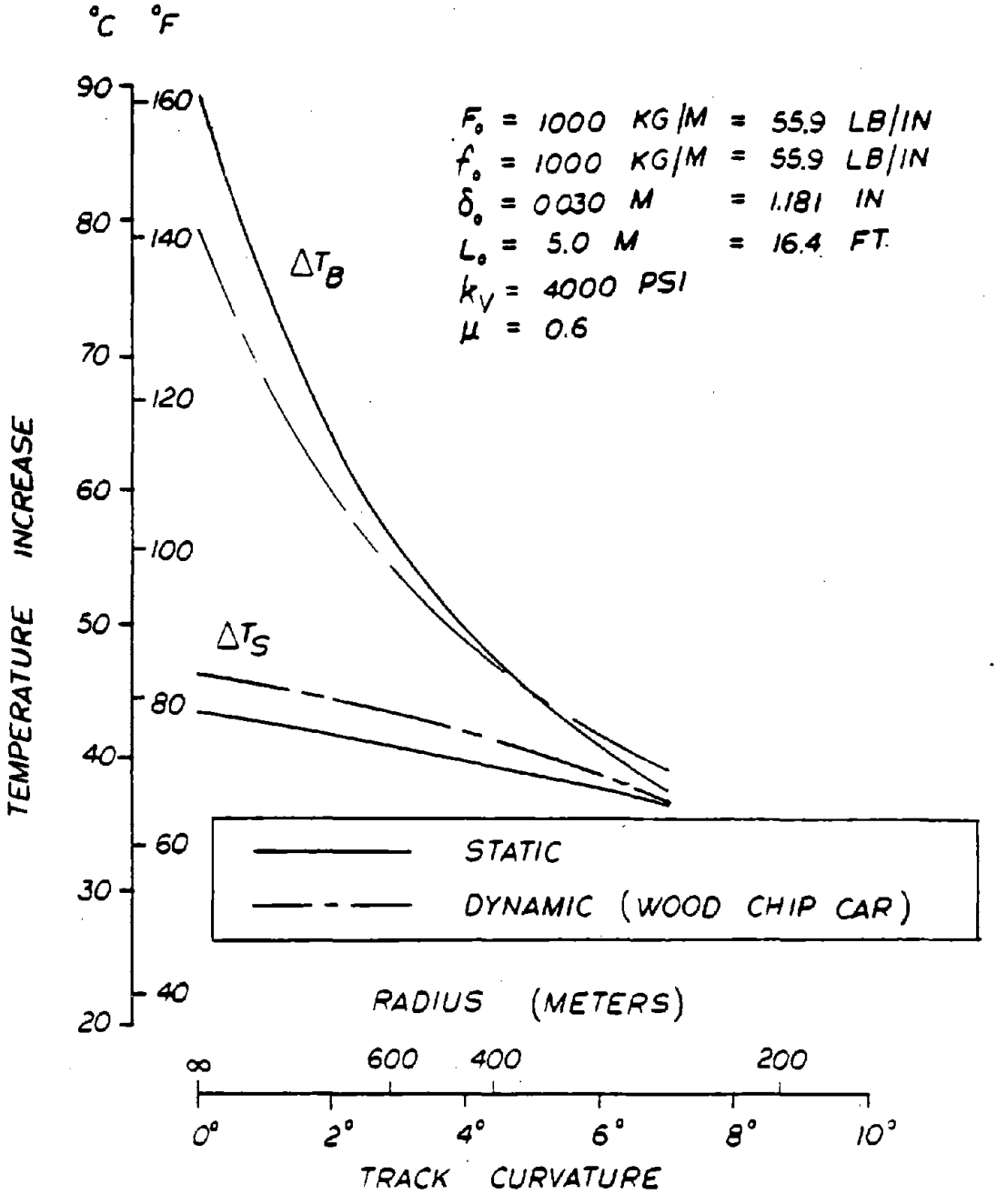

FIGURE 3.23 - STATIC VERSUS DYNAMIC (WOOD CHIP CAR) INFLUENCE ON SAFE TEMPERATURE INCREASE AND BUCKLING TEMPERATURE INCREASE FOR CURVED TRACKS

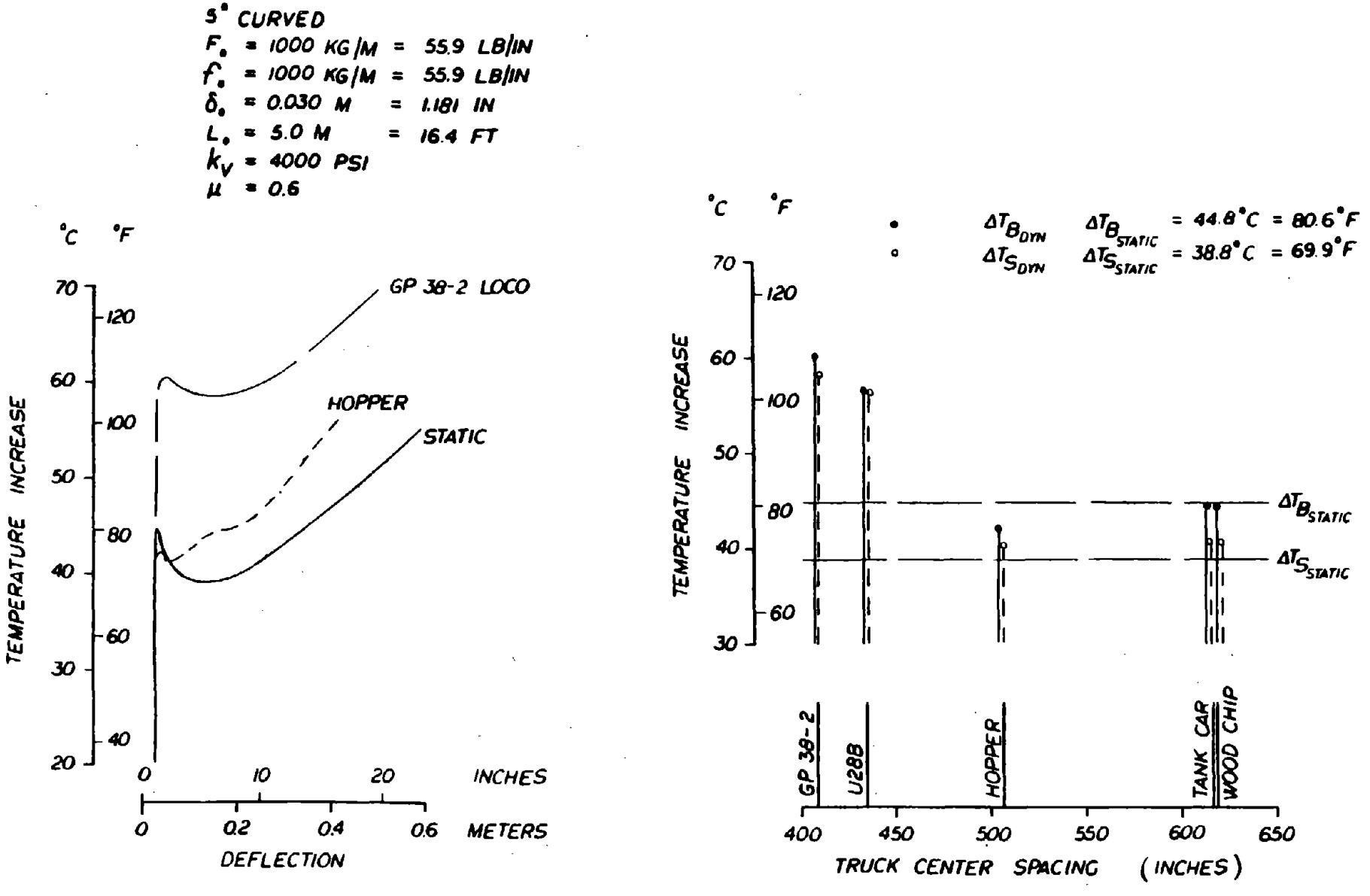

FIGURE 3.24 – EFFECT OF TRUCK CENTER SPACING ON SAFE TEMPERATURE INCREASE AND BUCKLING TEMPERATURE INCREASE

It should be noted that the track under the Covered Hopper Car is more vulnerable to progressive buckles compared to the static situation. This is particularly seen for curved track (curvature of 5^{o} or more, Fig. 3.21 and 3.22) for which no safe temperature exists if imperfections are of the order of 1 inch and larger. Clearly with smaller lateral resistances (that is, F_o less than 55.9 lb/in or 1000 kg/m), the dynamic buckling response for tight curves (curvatures greater than 5 degrees) is very sensitive to initial misalignments and may lead to progressive growth with increase in temperature.

Results are shown for the Wood Chip Car in Figure 3.23. The dynamic buckling temperature increases are lower than the static values. The dynamic safe temperature increases are slightly higher than the static safe values.

For the 5^{o} curved track with assumed imperfections, Figure 3.24 shows the dynamic and the static results for different cars. If the truck center spacing is small, both the safe and the buckling temperature increases will be increased due to the presence of the vehicle; if it is very large, the dynamic values tend to be equal to the static values. For some intermediate truck spacing, the dynamic buckling temperature increases can be significantly lower than the static values and progressive buckling can occur.

Figure 3.25 shows the test data obtained originally by the Hungarian railroad organization as reported by Kish in [15]. Both the static and the dynamic (moving car) test results for buckling temperature increases are shown. No safe temperature increases are shown, as these were not evaluated in the tests. The Hungarian test data are shown in Figure 3.25 as a percent difference between the static and the dynamic buckling temperature increases. The corresponding theoretical results for typical U.S. parameters are also shown. The theory predicts about 20% reduction in the buckling strength on the average for the Hopper Car whereas the test data are around 15%. Considering the fact that the experimental parameters are not really compatible with U.S. track and car parameters, this

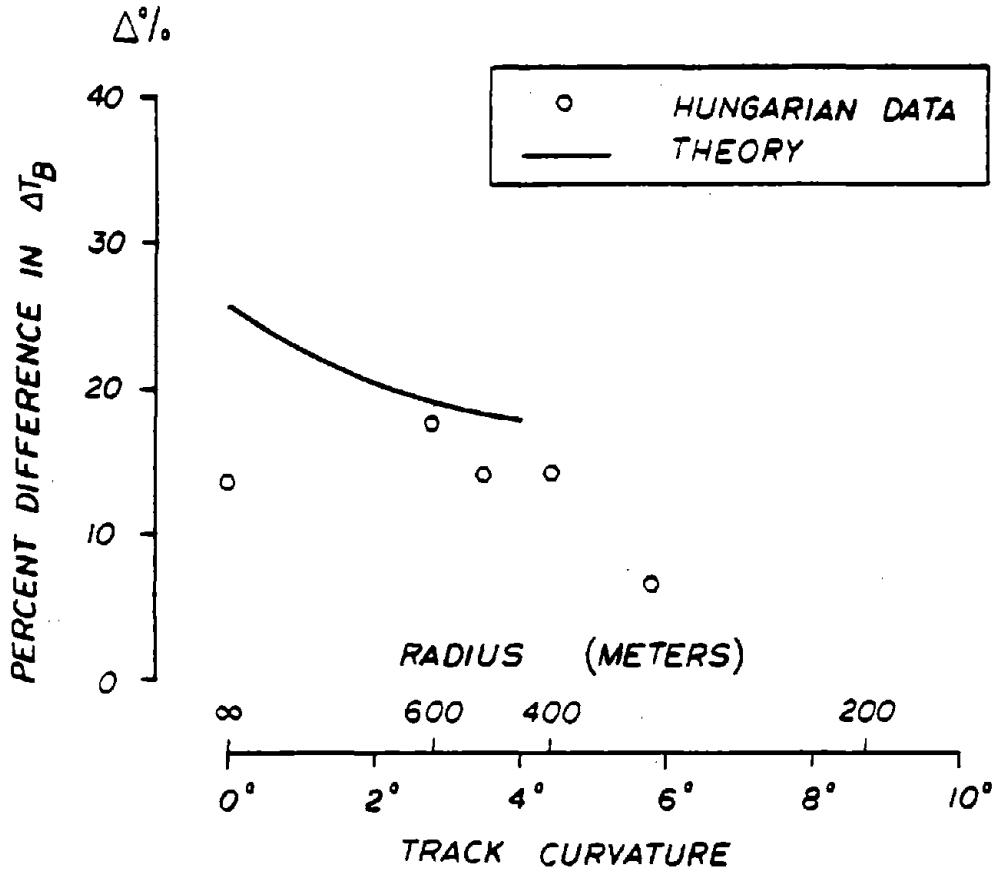

FIGURE 3.25 - COMPARISON OF HUNGARIAN EXPERIENTAL DATA TO THEORETICAL PREDICTION OF PERCENT DIFFERENCE IN BUCKLING TEMPERATURE INCREASE FOR CURVED TRACKS (STATIC VERSUS DYNAMIC)

agreement is reasonable.

3.3.3 Effect of Tie-Ballast Friction Coefficient

The tie-ballast friction coefficient is an important parameter contributing to track lateral resistance. Generally, the friction coefficient varies from 0.4 to 0.8, depending on the size and the type of ballast, amount of consolidation and roughness of tie bottom.

In Figure 3.26, the safe temperature increases are shown for varying values of the friction coefficient, for the GP38-2 locomotive and the Hopper Car. As one would expect, increasing the friction coefficient has a beneficial effect in both cases. In Figure 3.27, buckling temperature increases for both cars are shown. The buckling temperature for the GP38-2 Locomotive increases with the friction coefficient, but for the Hopper Car, it has no significant effect.

The insensitivity of the buckling temperature increase to the friction coefficient, in the case of the Hopper Car is due to the negligible change in the lateral resistance when the friction coefficient is varied. The upward reaction (due to the wheel loads) in the central wave is more or less equal to the track self weight, hence the contribution to the lateral resistance arising from tie-ballast friction is negligible.

3.3.4 Effect of Vertical Track Stiffness

It is clear that the track vertical foundation modulus, k_v, will have significant influence on the vertical deflection profile of the track and, hence, on the lateral resistance distribution. Eisenmann [17] has considered the track modulus as one of the most important parameters in his assessment of track buckling under the influence of vehicles.

The dynamic safe temperature increases for the GP38-2 locomotive and the Hopper Car are shown in Figure 3.28 for the range of 2,000 to 10,000 psi variation in track stiffness. The variation in the safe temperature increase is not significant. The dynamic safe temperature increases are

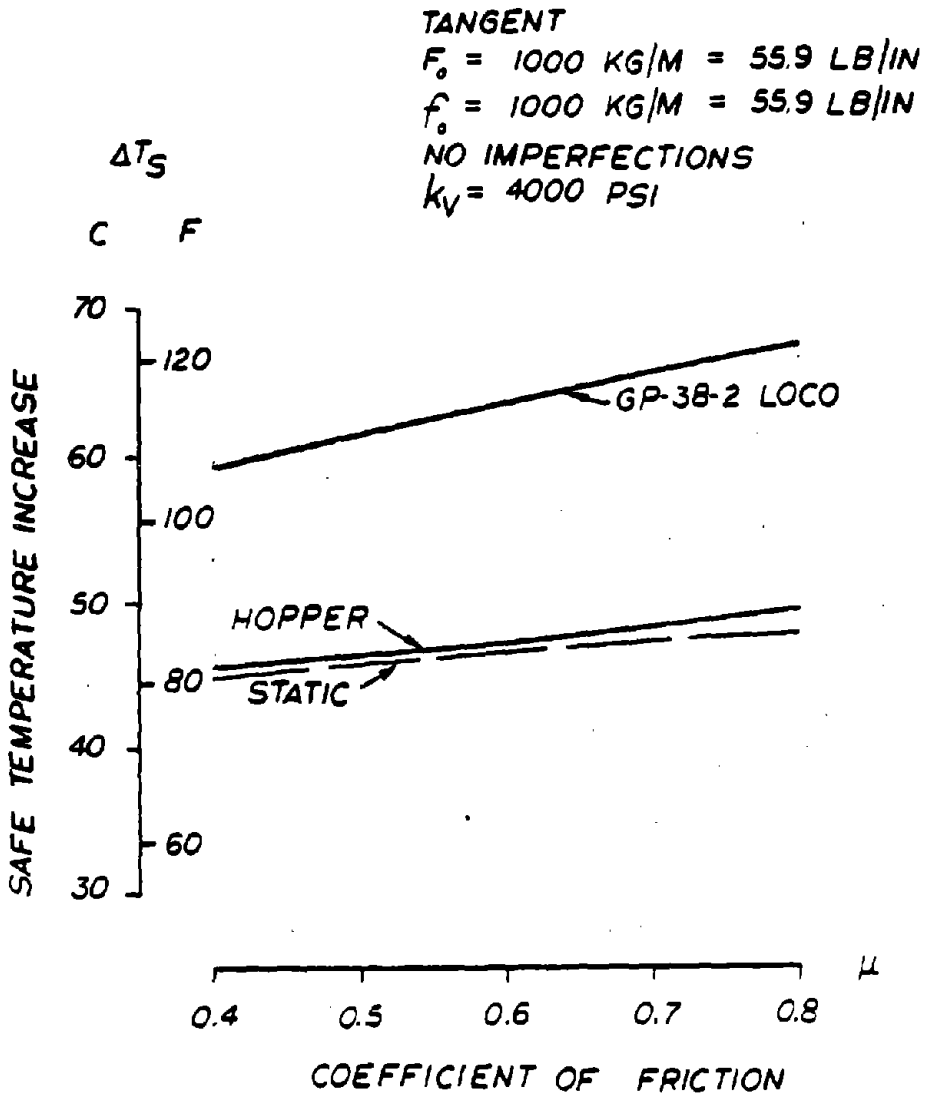

FIGURE 3.26 - EFFECT OF COEFFICIENT OF FRICTION ON SAFE TEMPERATURE INCREASE (GP38-2 LOCOMOTIVE VERSUS COVERED HOPPER CAR)

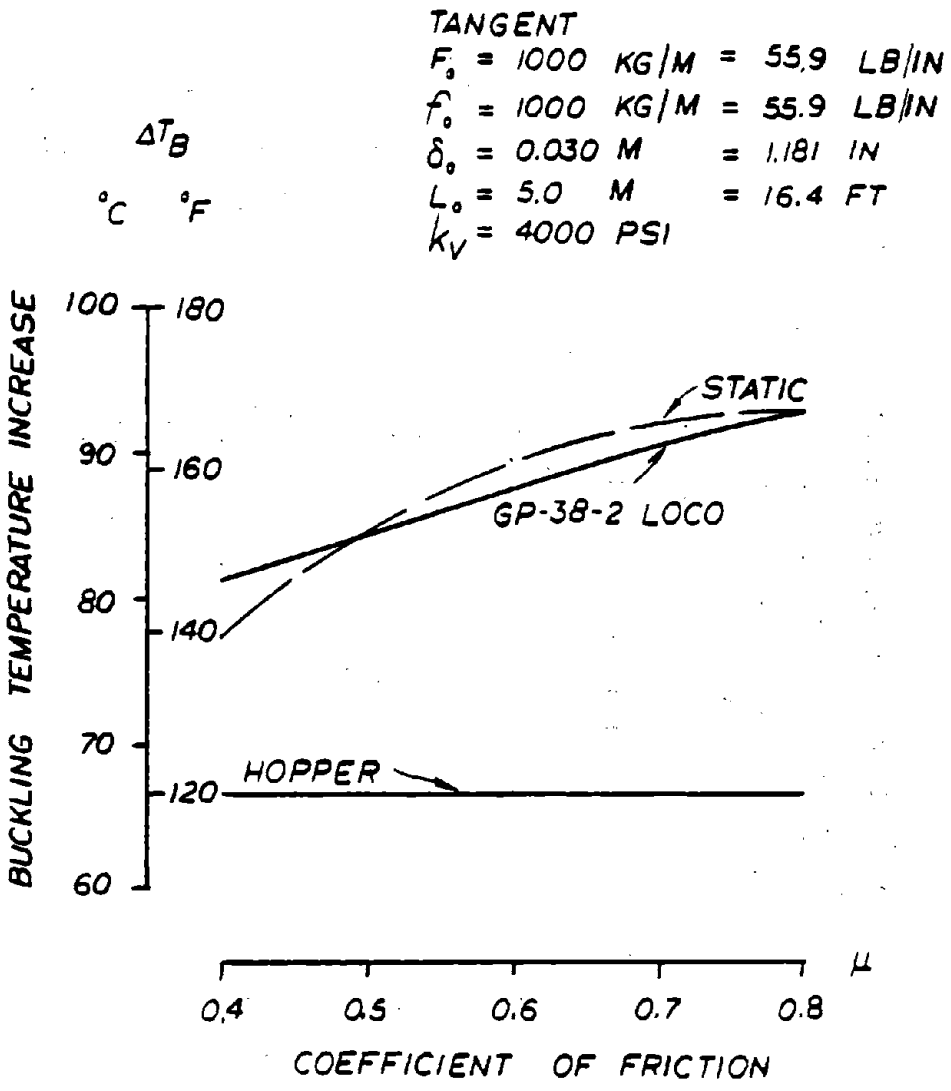

FIGURE 3.27 - EFFECT OF COEFFICIENT OF FRICTION ON BUCKLING TEMPERATURE INCREASE (GP38-2 LOCOMOTIVE VERSUS COVERED HOPPER CAR)

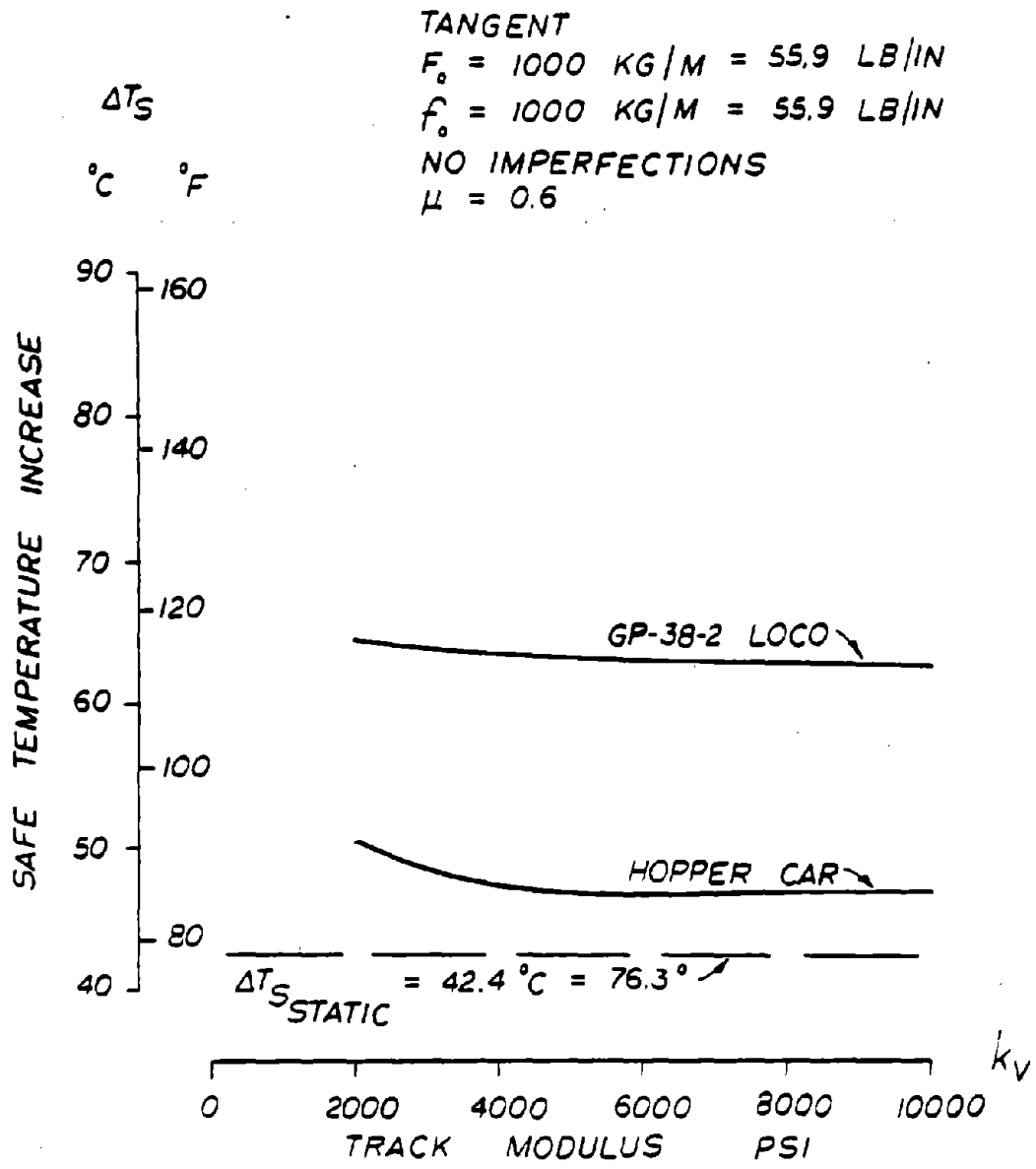

FIGURE 3.28 - EFFECT OF TRACK MODULUS ON SAFE TEMPERATURE INCREASE (GP38-2 LOCOMOTIVE VERSUS COVERED HOPPER CAR)

higher than the static values.

The dynamic buckling temperature increases for the GP38-2 Locomotive and the Hopper Car are shown in Figure 3.29. The locomotive exhibits a drop in its buckling temperature increase with increases in the track stiffness. The dynamic buckling temperature increases are generally lower than the static values.

For the Hopper Car, the buckling temperature values increase with increases in the track stiffness, k_v. However, these temperatures are still lower than the corresponding static buckling temperature values. This increased stability with increasing stiffness has also been alluded to by Eisenmann in [17].

3.3.5 Effect of Car Loading

Figure 3.30 shows the dependence of safe and buckling temperature increases for a Hopper Car versus its loading condition. It is interesting to note that the buckling temperature increase values decrease sharply up to about 1/4 full and thereafter remain constant. There is about 10% increase in the safe temperature increase from the empty to the fully loaded condition.

3.4 INFLUENCE OF PRECESSION WAVE

As stated in Section 3.3 upward bending deflections can occur in front of a locomotive (precession wave). Potential for buckling can be severe if the reduction in the lateral resistance caused by the precession wave is large enough. A detailed study of this influence has not been given urgent priority since the accident rate in front of the train consist seems to be much smaller than that of under the train [6]. (This seems to be the case for the European railroads also.) Hence, a rigorous analysis has not been performed on the precession wave as was done on the central wave. However, for completeness a brief discussion on the influence of the precession wave is included here.

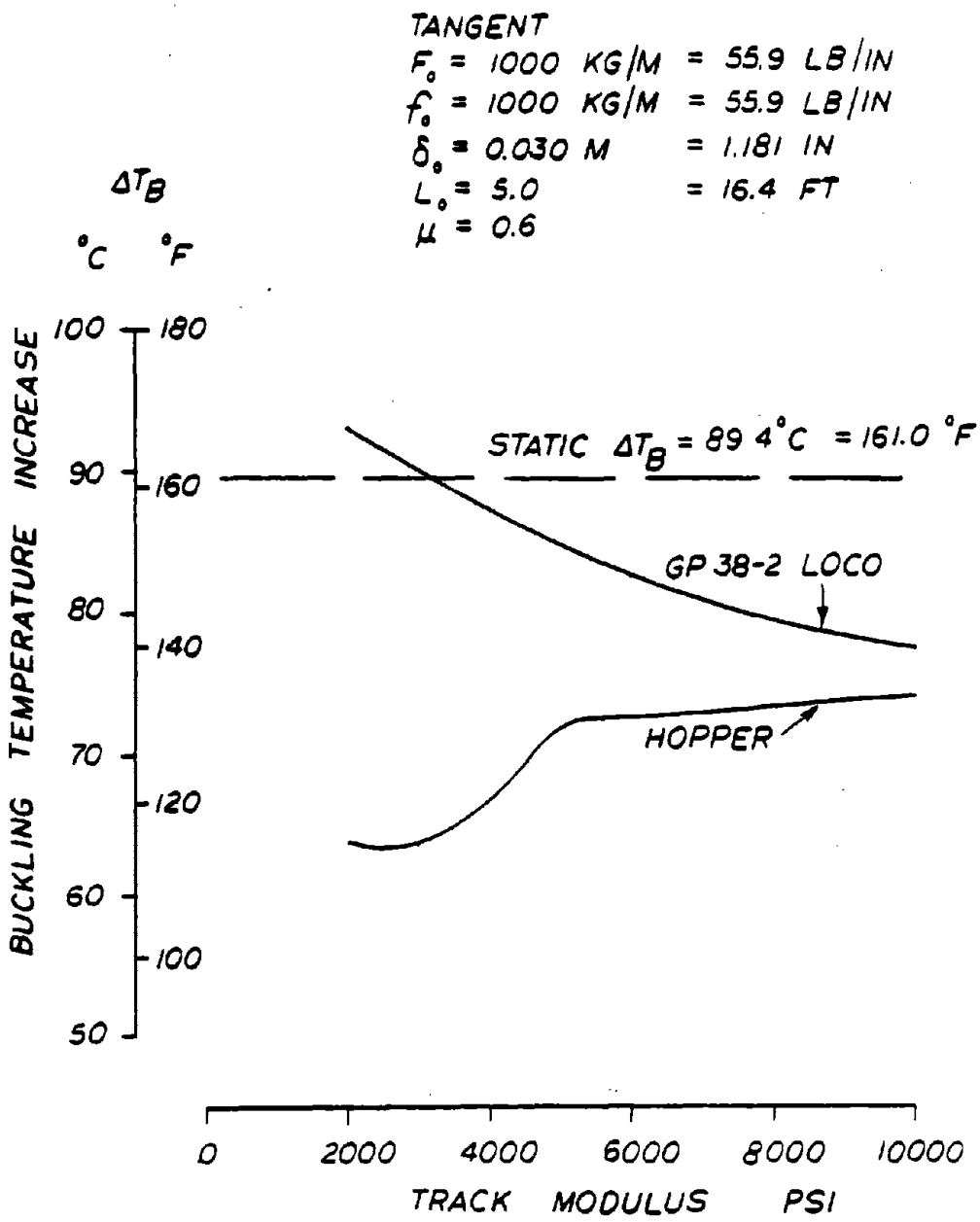

FIGURE 3.29 - EFFECT OF TRACK MODULUS ON BUCKLING TEMPERATURE INCREASE (GP38-2 LOCOMOTIVE VERSUS COVERED HOPPER CAR)

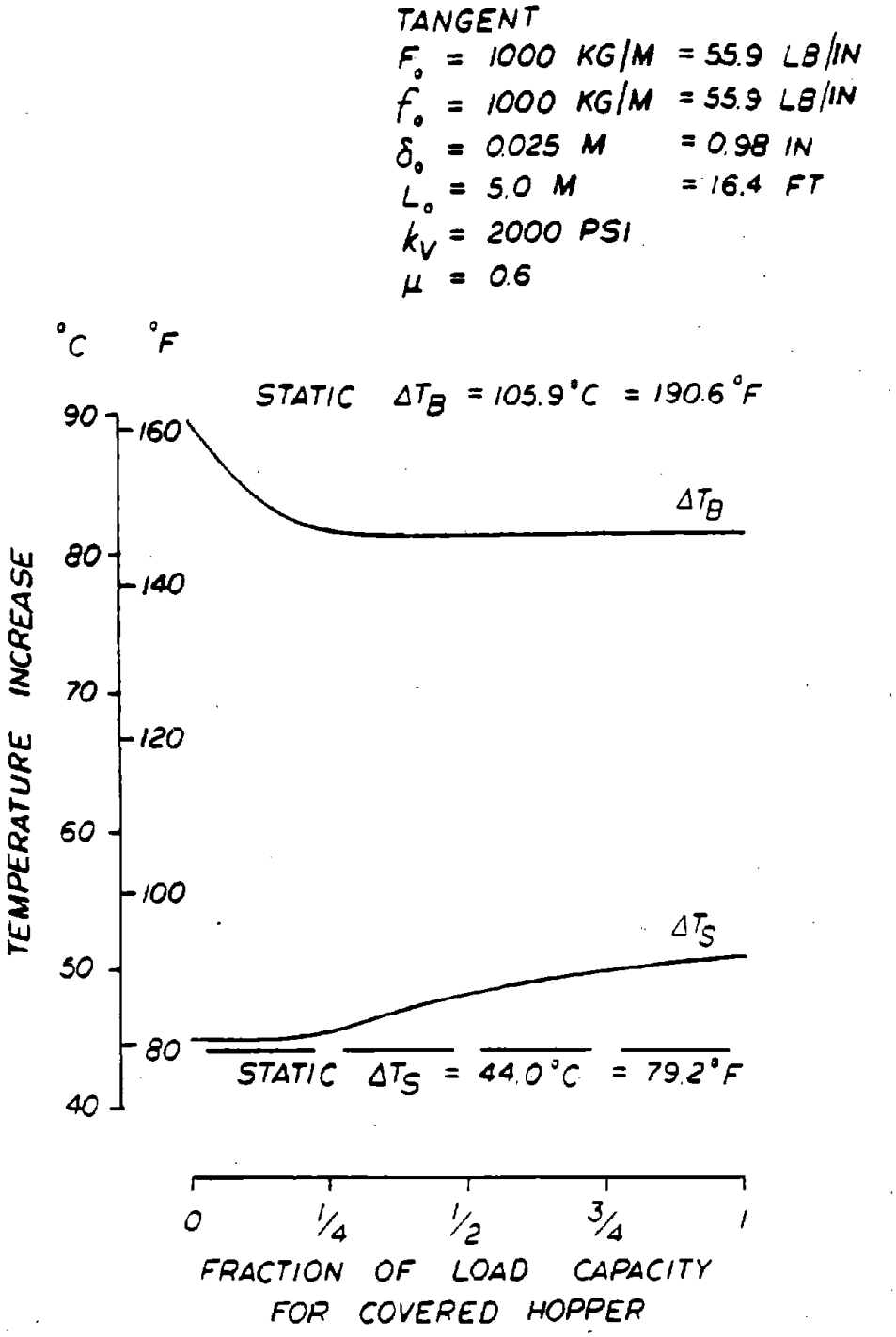

FIGURE 3.30 - EFFECT OF LOADING CONDITION FOR COVERED HOPPER CAR

Calculations have been carried out to examine the reduction in the lateral resistance in the precession wave zones of a GP38-2 locomotives and a Hopper Car. Figure 3.31 shows the lateral resistance distribution for the GP38-2 Locomotive. It can be seen that the loss of resistance in the precession wave zone is slightly more than it is in its central wave zone. Hence, the probability of buckling of the track in front of the locomotive is at least as much as under the locomotive. For a trailing hopper car in a consist (no caboose), the buckling potential due to the recession wave is much smaller than that due to the central wave beneath the hopper car, as seen from Figure 3.32. In any event, from these results one can infer that the critical uplift mechanism is the influence of the hopper car's central wave uplift. More tests are currently in progress to further quantify the effect of uplift on the dynamic buckling behavior of CWR track.

Mention must also be made here about certain experimental observations on track buckling in front of locomotives. In 1979, static pilot buckling tests were conducted by TSC at Chattanooga. Locomotives were stationed at the ends of the test track to provide adequate end restraints. No artificial imperfections were set in this experiment. The track buckled in front of one of the locomotives, hinting at a possible uplift influence. In 1980, Samavedam conducted some baseline dynamic buckling tests for British Rail in which a locomotive was run on the heated track at a slow speed which had an initial symmetric man-made imperfection. The imperfection grew with each pass of the locomotive. Eventually, the track buckled in front of the locomotive.

The foregoing experimental evidence seems to support the theoretical expectation that buckling due to the precession wave in front of the locomotive is a possibility.

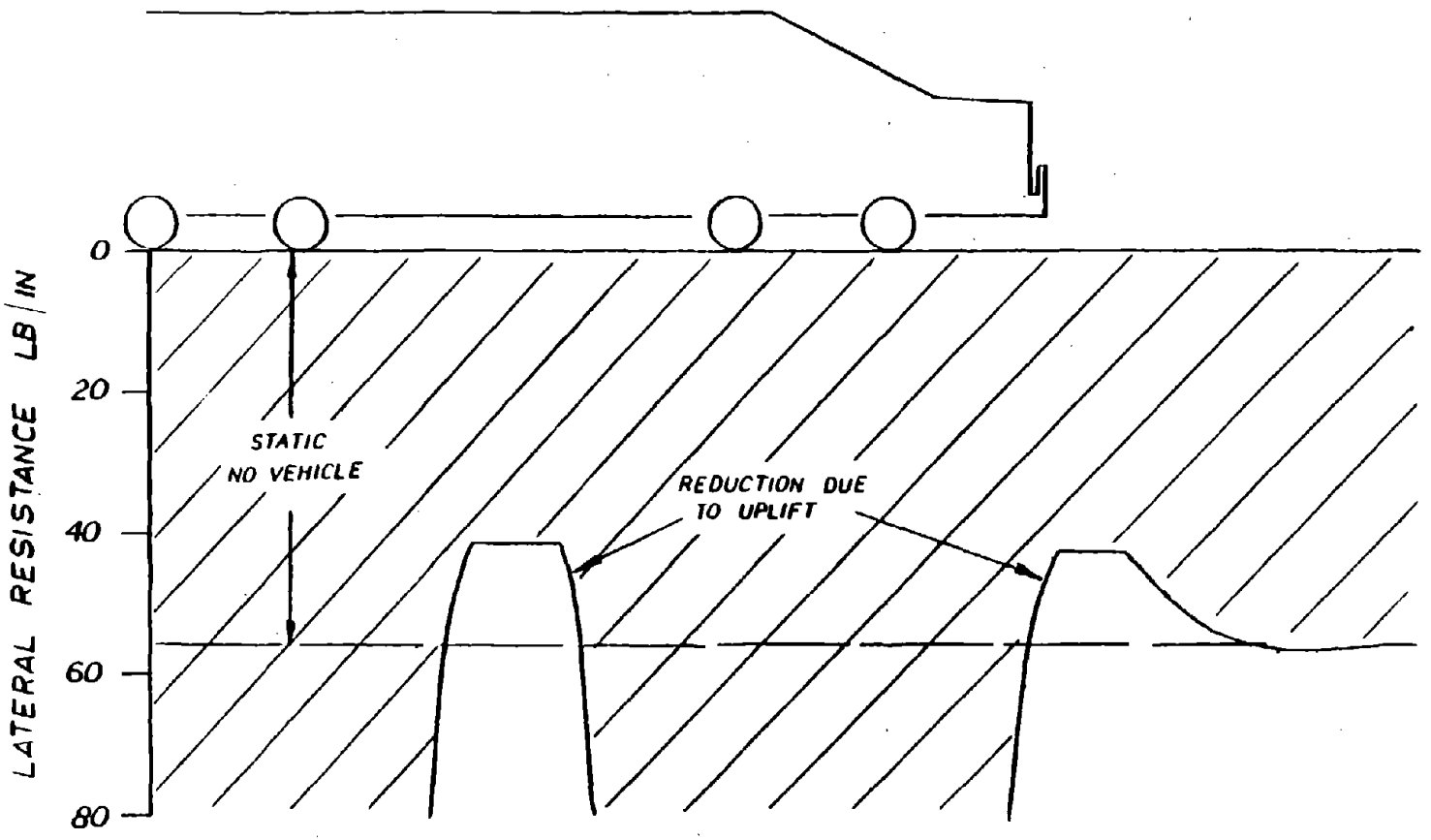

FIGURE 3.31 - LATERAL RESISTANCE DISTRIBUTION UNDER GP38-2 LOCOMOTIVE

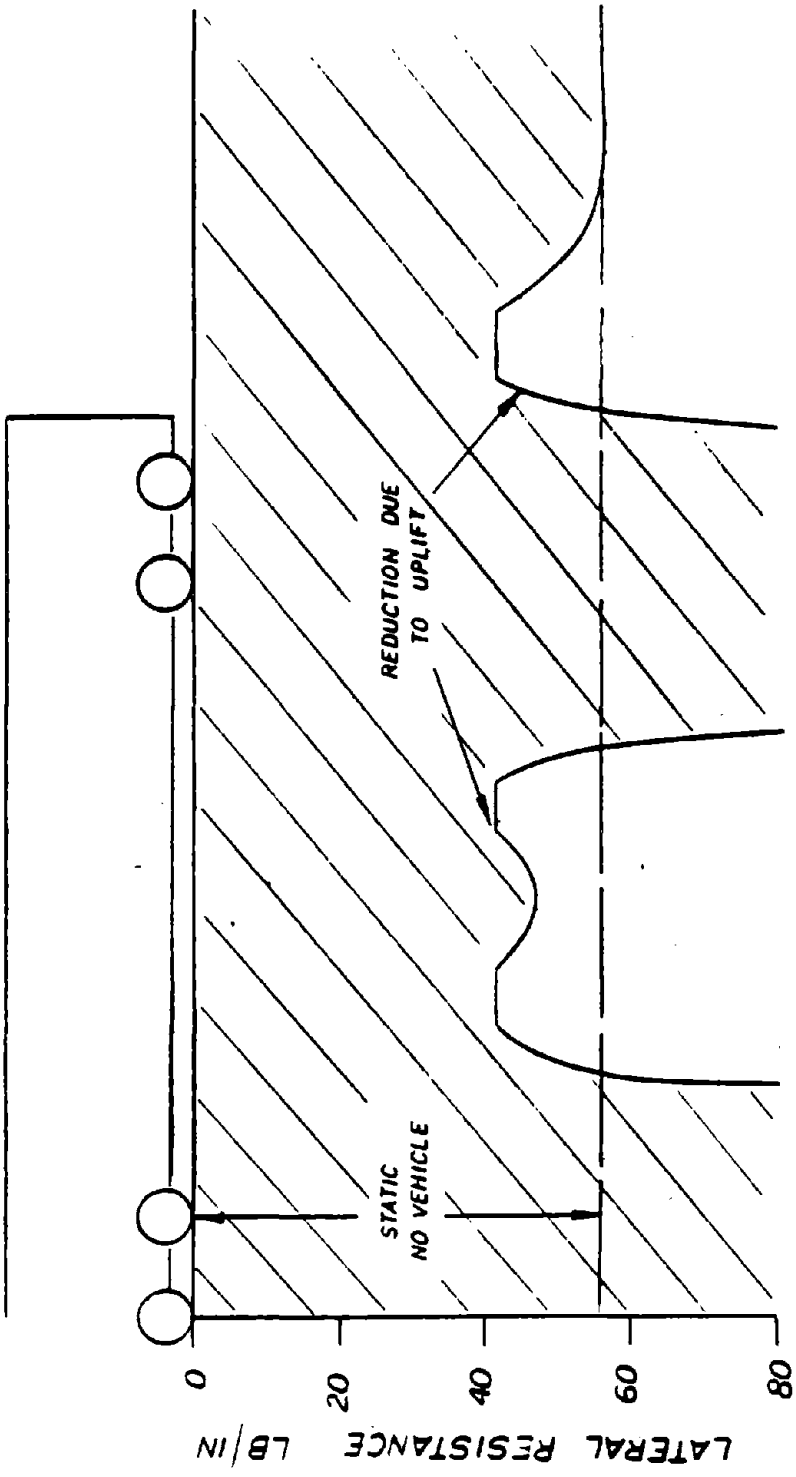

FIGURE 3.32 - LATERAL RESISTANCE DISTRIBUTION UNDER COVERED HOPPER CAR

4. CONCLUSIONS

(1) Three fundamental processes arising from vehicle loads affecting the thermal stability of continous welded rail tracks have been identified as summarized in Table 1, namely, the formation of lateral imperfections, the growth of lateral imperfections and the buckling of track in front of or under the train consist.

(2) Buckling directly underneath the wheels is unlikely unless the truck L/V (lateral/vertical load) ratios become larger than the coefficient of friction between the tie and the ballast which in general varies from 0.4 to 0.9. Truck L/V ratios of the order of 0.4 although not occurring too frequently can become dangerous on a poor ballast. The vertical wheel loads tend to stablize the track in the vicinity of wheels, whereas the lateral load tends to deform the track laterally and thus enhance the buckling potential. The critical truck L/V ratio is equal to the coefficient of friction between the ballast and tie.

(3) The vertical wheel loads can produce negative (upwards) bending deflections at some distance away from the wheels. Three different zones of influence have been identified for isolated two truck cars: a recession wave behind the trailing truck, a precession wave in front of the leading truck and a central wave in between the two trucks. The bending deflections when superimposed on the uniform deflection due to self weight will indicate whether or not a track lifts off the ballast bed in these three zones. Generally, the lift-off is less than 0.01 inches for typical tracks, and is dependent upon track stiffness, vertical load, truck center spacing and track weight.

(4) The maximum reduction in lateral resistance will occur in the lift-off zone. This reduction can be of the order of 40% when complete loss of the base friction occurs.

(5) Truck center spacing has an influence on the safe temperature increase values. For short cars and GP38-2 type locomotives the safe temperature increases are significantly higher than the static values. For "long" cars the dynamic safe temperature increases are of the same order as the static values, if the track is assumed to be free of imperfections.

(6) The dynamic buckling temperature decreases with increasing truck center spacing. For the GP38-2 type locomotives the buckling temperatures are generally higher than the static values. For "long" cars (hopper cars, tank and wood chip cars), the dynamic buckling temperatures are lower than the static values by more than 20-30%.

(7) For the GP38-2 type locomotives buckling potential in front of (precession wave) and underneath the locomotive (central wave) appear to be equal. However, for a consist of long cars, the central wave regions under each car are more susceptible to buckling than the single precession wave in front of the locomotive. This is due to the longer central wave length and the recurring lifting wave induced by each wheel passage. Hence, buckling under the train is more likely than in front of the locomotive.

(8) The track vertical stiffness has an influence on track buckling in the lateral plane in the presence of vehicle loads since the track modulus influences the extent of the uplift regime. In general, tracks under locomotives tend to exhibit an increase in buckling strength with a reduction in track stiffness, while tracks beneath long cars exhibit a decrease in buckling strength with a reduction in track stiffness as shown in Figure 3.29. This is a consequence of variation in the respective lengths of uplift waves as influenced by vertical track stiffness.

(9) This study has revealed that the dynamic buckling temperature is more important than the static buckling temperature for CWR safety point of view. Furthermore, the track (particularly curved track) is much more imperfection sensitive dynamically than statically (without vehicle).

In fact, in the presence of imperfections, the track may not exhibit a "dynamic safe temperature", although it may show a static safe temperature. These findings may impact the CWR safety specifications.

(10) In view of the above, in addition to requiring a minimum allowable safe temperature increase, a proper safety criterion for buckling prevention must also require the existence of a dynamic buckling temperature increase within some stipulated margin of safety. This latter requirement would ensure against progressive buckling.

5. RECOMMENDATIONS

(1) It is important to understand quantitatively the components contributing to the lateral resistance of the track. It is known that there are three basic components which comprise the track lateral resistance as discussed in Appendix A, namely:

$$F = F_e + F_s + F_b$$

where F_e = shoulder or end resistance, F_s = side friction, and F_b = base friction between tie bottom and the ballast. The respective values of each of these components for U.S. track are not known. For European track (wood ties), these values can typically be: $F_e = F_s =$ 10.0 lb/in, and F_b = 13.5 lb/in for a freshly tamped track. For a consolidated track, there is limited information available. This information is needed for better estimates of loss of resistance under precession and central waves.

(2) The formation and the growth of imperfections need to be examined as they are closely related to track buckling under the influence vehicles.

(3) The theoretical aspects and analysis predictions require field test verification. Specifically, the "long" versus "short" car influence (uplift) and truck L/V influence need rigorous test validation. Detailed test requirements definitions for the conduct of such dynamic buckling tests is available in [18].

(4) In the presence of imperfections, vehicles such as the Hopper Car have significantly reduced buckling temperatures. For curves with low lateral resistance, the buckling can be progressive, and there is no dynamic safe temperature. Application of safe temperature increase criterion may become problematic in such situations. A suitable safety criterion along the lines of conclusion (10) needs to be developed and validated.

APPENDIX A

DETERMINATION OF TRACK LATERAL RESISTANCE UNDER VEHICLE LOADS

There are two basic problems in the determination of track lateral resistance under vehicle loads:

- o Determination of vertical reaction on ties (pressure distribution between ties and ballast)
- o Evaluation of lateral resistance contribution of the tie base friction from the knowledge of vertical reaction distribution.

These two problems will be discussed in detail here.

A.1 DETERMINATION OF VERTICAL REACTION

The most commonly used "standard" analysis assumes the ballast to behave as a Winkler foundation, i.e., the ballast reaction on ties is directly proportional to the vertical deflection. The vertical deflection is the sum total due to the wheel loads and the self weight of the track (ties, fasteners plus rail). The vertical downward deflection v_o, due to self weight (lb/in) is given by

$$v_o = q/k_v \tag{A-1}$$

where k_v= foundation modulus (lb/in^2)

The track foundation modulus can vary depending on the ballast type, depth, consolidation level etc. Practical values are in the range of 2000 to 6000 psi.

Bending deflections due to wheel loads can be determined using the Hetenyi beam analysis [13]. For example in the case of a single wheel load P, at the origin, x = 0, the vertical deflection profile is given by

$$v_1 = \frac{P_1 \lambda}{2k} F_1 (\lambda x) \tag{A-2}$$

$$\text{where } F_1 (\lambda x) = e^{-\lambda x} (\cos \lambda x + \sin \lambda x) \tag{A-3}$$

$$\lambda = \left(\frac{k_v}{4EI_y}\right)^{1/4} \tag{A-4}$$

For multiple wheel loads, superposition is used in the standard linear analysis.

The net deflection is obtained by adding the self weight deflection v_o to the wheel load deflection v_l. This may lead to negative deflections (upwards) over some length of rails, representing "uplift of track", which implies tensile reaction between ties and ballast. Since tensile stresses cannot be borne by the ballast, improved models have been developed in the literature.

For example, Kerr and Bassler [16] performed an analysis of "tensionless" foundation model, which assumes zero foundation modulus, (hence zero reaction) in the uplift regions. Using this model comparison studies for a single and two axle truck loads against the standard analysis indicate that the lengths of uplift zones are not significantly different, although the lift off amplitudes are. Therefore setting vertical reaction in the uplift region as computed in the standard analysis equal to zero seems to be adequate for an approximate estimation of lateral resistance distribution under the vehicle loads.

A.2 EVALUATION OF LATERAL RESISTANCE

It is known that the lateral resistance of a tie consists of three components:

- Base friction F_b, at the interface between the tie bottom and ballast
- Side friction, F_s, between the tie sides and the ballast
- and shoulder resistance, F_e, at the ends of tie due to ballast shoulder

Thus the total resistance F_o is given by

$$F_o = F_b + F_s + F_e \qquad \text{(A-5)}$$

In the case of static buckling theory, the decomposition of the resistance in the three components is not needed; however, for the dynamic buckling theory, the proportions are very important. This is because the base friction varies with the vertical reaction due to vehicle loads. If we assume that the friction force is proportional to the reaction, in the Coulomb sense, we find that

$$F_o \text{ (static)} = \mu Q + F_s + F_e$$

where μ = friction coefficient, and Q is the total self weight of the track (rails, ties, tie plates, etc.)

In the presence of vehicles, the dynamic lateral resistance outside the uplift zone is given by

$$F_o \text{ (dynamic)} = \mu(Q + R_v) + F_s + F_e \qquad \text{(A-7)}$$

where R_v = vertical reaction taken positive upwards on ties and is equal to kv where v is deflection due to wheel loads. In the uplift zone, we take $Q + R_v = 0$, hence

$$F_o \text{ (dynamic)} = F_s + F_e \qquad \text{(A-8)}$$

It is clear that the dynamic resistance cannot be determined without any knowledge of proportions of the three components in the static situations. Some data is available in the European literature [19,20], however. According to some of the experimental data collected by the Research and Development Division of British Rail the proportions of the three components are in the following range

		Wood Tie	Concrete Tie
F_b, Base friction	=	29-47%	30-58%
F_s, Side friction	=	27-65%	30-54%
F_e, Shoulder resistance	=	5-25%	4-28%

In the work presented here, the following values have been assumed for typical tamped wood tie track with average tie center spacing of 20 inches:

CASE NO.	TRACK WEIGHT lb/in(kg/m)	FRICTION COEFFICIENT	F_b, BASE FRICTION lb/in(kg/m)	F_s, SIDE FRICTION lb/in(kg/m)	F_e, SHOULDER RESISTANCE lb/in(kg/m)	F_o TOTAL lb/in(kg/m)
1	24.0	0.6	14.0	11.2	8.4	33.5
	(429)		(250)	(200)	(150)	(600)
2	24.0	0.6	14.0	27.9	14.0	55.9
	(429)		(250)	(500)	(250)	(1000)

In case 1, the proportions of the three components are 42:33:25, while in case 2 the proportions are 25:50:25. It must be noted that no data is available for U.S. track to confirm the foregoing assumed proportions.

APPENDIX B

THEORETICAL EQUATIONS FOR INCLUDING EXTERNAL LOAD EFFECTS IN THE LATERAL STABILITY ANALYSES

A versatile method of analyzing the lateral stability of continuous welded rail track has been developed by Samavedam [2]. This method is capable of analyzing tracks with varying radii of curvature, lateral misalignments, and nonlinearities in resistance characterizations (lateral, longitudinal, and torsional resistances). In this appendix, the static theory developed by Samavedam is modified to include effects of applied vertical and/or lateral loads. The modifications described in this appendix begin with the case of a single axle load on the track and methods are discussed to extend the modifications to cases for a single truck load and a two truck (vehicle) load. Only one buckling mode shape, mode I, will be discussed here.

The assumptions made in the buckling analyses include:

- lateral and longitudinal resistances are constant at all displacement levels
- torsional resistance is neglected
- longitudinal resistance in the buckled zone is neglected
- lateral misalignments are assumed to be sinusoidal

From the "static" theory the differential equation describing tangent track is:

$$EIw'''' + \bar{P}w'' = -F_o - \bar{P}w_o'' \qquad \text{(B-1)}$$

where EI = flexural rigidilty in the lateral plane

$\bar{P}$ = rail compressive force in the buckled zone

F_o = constant value of lateral resistance

w_o = misalignment in track

Fourier analysis has been used as a solution technique by defining:

$$w(x) = \sum_{1,3,5\ldots}^{\infty} A_m \cos\left(\frac{m\pi x}{2L}\right) \tag{B-2.1}$$

$$F_o(x) = \sum_{1,3,5\ldots}^{\infty} a_m \cos\left(\frac{m\pi x}{2L}\right) \tag{B-2.2}$$

$$w_o''(x) = \sum_{1,3,5\ldots}^{\infty} b_m \cos\left(\frac{m\pi x}{2L}\right) \tag{B-2.3}$$

and boundary conditions as:

$$w' = w'' = 0 \quad \text{at } x = 0 \tag{B-3.1}$$

$$w = w' = w'' = 0 \quad \text{at } X = \pm L \tag{B-3.2}$$

where L is the buckled wavelength.

In general, the Fourier coefficients are found from

$$a_m = \frac{2}{L} \int_o^L F_o(x) \cos\left(\frac{m\pi x}{2L}\right) dx \tag{B-4.1}$$

$$b_m = \frac{2}{L} \int_o^L w''(x) \cos\left(\frac{m\pi x}{2L}\right) dx \tag{B-4.2}$$

$$A_m = \frac{-(a_m + \bar{P} b_m)}{\left[EI\,(m\pi/2L)^4 - \bar{P}\left(\frac{m\pi}{2L}\right)^2\right]} \tag{B-4.3}$$

The integration of these Fourier coefficients has been carried out for the static case and can be found in References 2 and 3. The complete solution is obtained (noting that L is an unknown) by stipulating that

$$w'(L) = -\sum_{1,3,5\ldots}^{\infty} A_m \left(\frac{m\pi}{2L}\right) \sin\left(\frac{m\pi}{2}\right) = 0 \tag{B-5}$$

The temperature* for straight track theory is calculated from

$$T = \left\{P + f_o L \left[-1 + \sqrt{1 + \frac{2AEZ}{f_o L^2}}\,\right]\right\} / AE\alpha \tag{B-6.1}$$

where

$$Z = \frac{L}{2}\left[1/2 \sum_{1,3,5\ldots}^{\infty} A_m^2 \left(\frac{m\pi}{2L}\right)^2 - \sum_{1,3,5\ldots}^{\infty} A_m b_m\right] \tag{B-6.2}$$

*It is assumed that the longitudinal resistance in the breathing zone has not been significantly altered due to the weight of the vehicle. This assumption is not strictly valid. A correction for this can be made as shown later.

Curved Track Equations

The equation for the "static" curved track theory are quite similar in form to the tangent track equations:

$$\frac{EI}{R^4}\overset{\cdots\cdot}{w} + \frac{\bar{\Gamma}\overset{\cdot\cdot}{w}}{R^2} = -F_o + \frac{\bar{P}}{R} - \frac{\bar{P}\overset{\cdot\cdot}{w}_o}{R^2} \qquad \text{(B-7)}$$

The Fourier analysis proceeds by defining

$$w(\theta) = \sum_{1,3,5\ldots}^{\infty} A_m \cos\left(\frac{m\pi\theta}{2\phi}\right) \qquad \text{(B-8.1)}$$

$$\left(F_o - \frac{\bar{P}}{R}\right) = \left(F_o - \frac{\bar{P}}{R}\right) \sum_{1,3,5\ldots}^{\infty} a_m \cos\left(\frac{m\pi\theta}{2\phi}\right) \qquad \text{(B-8.2)}$$

$$\frac{\bar{P}}{R^2}\overset{\cdot\cdot}{w}_o(\theta) = \frac{\bar{P}}{R^2} \sum_{1,3,5\ldots}^{\infty} b_m \cos\left(\frac{m\pi\theta}{2\phi}\right) \qquad \text{(B-8.3)}$$

where the Fourier coefficients are found from

$$a_m = \frac{2}{\phi}\int_o^{\phi} \cos\left(\frac{m\pi\theta}{2\phi}\right) d\theta \qquad \text{(B-9.1)}$$

$$b_m = \frac{2}{\phi}\int_o^{\phi} \dot{w}_o \cos\left(\frac{m\pi\theta}{2\phi}\right) d\theta \qquad \text{(B-9.2)}$$

$$A_m = -\left[\left(F_o - \bar{P}/R\right) a_m + \left(\bar{P}/R^2\right) b_m\right] / \left[EI/R^4\left(\frac{m\pi}{2\phi}\right)^4 - \frac{\bar{P}}{R^2}\left(\frac{m\pi}{2\phi}\right)^2\right] \qquad \text{(B-9.3)}$$

Again, the complete solution is obtained by stipulating that

$$\dot{w}\Big|_{\theta=\phi=o} = \sum_{1,3,5\ldots}^{\infty} A_m\, m \sin\left(\frac{m\pi}{2}\right) = 0 \qquad \text{(B-10)}$$

The temperature equation for the curved track case is the same as for tangent track, equation B-6.1, with a variation in the value of Z as follows:

$$Z = \sum_{1,3,5\ldots}^{\infty} \left[\frac{2\phi}{m\pi R} \sin\left(\frac{m\pi}{2}\right) A_m + \left(\frac{m\pi}{R}\right)^2 \frac{1}{16\phi} A_m^2 - \frac{A_m b_m \phi}{2R^2}\right] \qquad \text{(B-11)}$$

The foregoing equations have been used in the "static" buckling analysis and require a few changes in order to apply them to the case for external load-

ing. In the theory presented here, the only difference between the "static" and "dynamic" theory is in the assumption for track lateral resistance as described in Appendix A. Therefore, the "dynamic" theory requires the solution of the Fourier Series coefficients involving the lateral resistance function; namely, equations B-4.1 for tangent track and B-9.1 for curved track.

The Fourier Series coefficients have been expressed as integrals which can be evaluated exactly using standard tables (e.g., Standard Mathematical Tables, 15th edition, edited by S.M. Selby, The Chemical Rubber Co., 1967). In general, the solution of these Fourier Series coefficients requires evaluation of the following:

$$a_m = \frac{2}{L} \int_o^L F(x) \cos \left(\frac{m\pi x}{2L}\right) dx \qquad \text{(B-12)}$$

where F(x) = track lateral resistance function.

As an example, the single axle load case would proceed as follows:

$$a_m = \frac{2}{L} \int_o^L F(x) \cos \left(\frac{m\pi x}{2L}\right) dx \qquad \text{(B-13)}$$

$$= \frac{2}{L} F_o \int_o^L \cos \left(\frac{m\pi x}{2L}\right) dx$$

$$+ \frac{2}{L} \frac{P\lambda\mu}{2} \int_o^L F_1(\lambda x) \cos \left(\frac{m\pi x}{2L}\right) dx$$

$$= \frac{4F_o}{m\pi} \sin \left(\frac{m\pi}{2}\right) + \frac{\mu P\lambda}{2} \int_o^L F_1(\lambda x) \cos \left(\frac{m\pi x}{2L}\right) dx$$

$$= a_{m1} + a_{m2}$$

Note that the a_{m1} term is equal to a_m for the case where no vertical loading is present. Expansion of the a_{m2} term continues as:

$$a_{m_2} = \frac{\mu P\lambda}{L} \left[\int_o^L e^{-\lambda x} \cos \lambda x \cos \left(\frac{m\pi x}{2L}\right) dx \right.$$

$$\left. + \int_o^L e^{-\lambda x} \sin \lambda x \cos \left(\frac{m\pi x}{2L}\right) dx \right] \qquad \text{(B-14)}$$

As discussed earlier, the a_{m2} term can be solved using the CRC Standard Mathematical tables which evaluate these integrals exactly as given in equations B-15 and B-16.

$$\int e^{ax} \cos bx \cos cx \, dx = \frac{e^{ax}[(b-c) \sin (b-c)x + a \cos (b-c) x]}{2[a^2 + (b-c)^2]}$$

$$+ \frac{e^{ax}[(b+c) \sin (b+c) x + a \cos (b+c) x]}{2[a^2 + (b+c)^2]} \qquad \text{(B-15)}$$

$$\int e^{ax} \sin bx \cos cx \, dx = \frac{e^{ax}[a \sin (b-c) x - (b-c) \cos (b-c)x]}{2[a^2 + (b-c)^2]}$$

$$+ \frac{e^{ax}[a \sin (b+c) x - (b+c) \cos (b+c) x]}{2[a^2 + (b+c)^2]} \qquad \text{(B-16)}$$

When multiple vertical loads are applied and when there is no lift of the solution of the Fourier series coefficients involving the lateral resistance function is quite similar. Recall from Appendix A that the principle of superposition is used in the cases where multiple vertical loads are present. Therefore, the expression equivalent to equation B-13 for multiple loads becomes longer. In these cases, the CRC tables can be used (i.e., equations B-15 and B-16) along with an additional integral which results from the longer expression in equation B-13:

$$\int e^{ax} \sin bx \sin cx \, dx = \frac{e^{ax}[(b-c) \sin(b-c)x + a \cos (b-c)x]}{2[a^2 + (b-c)^2]}$$

$$- \frac{e^{ax}[b+c) \sin (b+c)x + a \cos (b+c)x]}{2[a^2 + (b+c)^2]} \qquad \text{(B-17)}$$

The preceeding discussion has focussed on the case where no lift off of the track has occurred. As discussed in Appendix A, however, the track can experience lift off and the calculation of the Fourier Series coefficient in this case proceeds as follows:

$$a_{m_2} = \frac{2}{L} \int_{\ell_1^*}^{\ell_2^*} F^* \cos \left(\frac{m\pi x}{2L}\right) dx \qquad \text{(B-18.1)}$$

$$= \frac{4F^*}{m\pi} \sin \left(\frac{m\pi x}{2L}\right) \Bigg|_{\ell_1^*}^{\ell_2^*} \qquad \text{(B-18.2)}$$

$$= \frac{4F^*}{m\pi} \left[\sin \left(\frac{m\pi \ell_2^*}{2L}\right) - \sin \left(\frac{m\pi \ell_1^*}{2L}\right)\right] \qquad \text{(B-18.3)}$$

where $F^* = F_s + F_e$ = lateral resistance in the uplift zone (see Appendix A).

ℓ_1^*, ℓ_2^* = dimensions of uplift zone.

The limits of integration in the above expressions are lengths of the uplift zone which are highly dependent upon the magnitude of the applied vertical loading, the spacing of these loads if multiple loads are applied, and the track foundation modulus. As discussed in the text, the vertical load case presents scenarios where uplift regions can be created by vertical loading between the two trucks. Depending on the truck center spacing there may be no uplift, one uplift zone or two uplift regions between the two trucks. When there is lift off these uplift regions must be defined and the a_{m2} term must be integrated over the defined regions using the appropriate (i.e., uplift versus no uplift) expression for the Fourier Series coefficient.

When lateral loads are considered, the solution of the Fourier Series is again affected. In these cases the Fourier Series coefficient becomes

$$a_m = a_{m1} + a_{m2} + a_{m3} \qquad \text{(B-19)}$$

where a_{m1} = "static" contribution

a_{m2} = vertical loading contribution

a_{m3} = lateral loading contribution

Careful consideration must be taken when the multiple lateral loads are applied since the assumed buckling length may or may not be within the range where the lateral loads are applied (see Figures B.1 and B.2). The a_{m3} term for the lateral load cases considered in this document is now summarized and given as follows (note the F_H is the value of the applied lateral load and L is the buckled length):

Single Axle Case

$$a_{m3} = -\frac{F_H}{L} \qquad \text{(B-20.1)}$$

Truck Load Case

$$a_{m3} = \begin{cases} 0 & \text{for } L \leq S \\ \frac{2F_H}{L} \cos\left(\frac{m\pi S}{2L}\right) & \text{for } L > S \end{cases} \qquad \text{(B-20.2)}$$

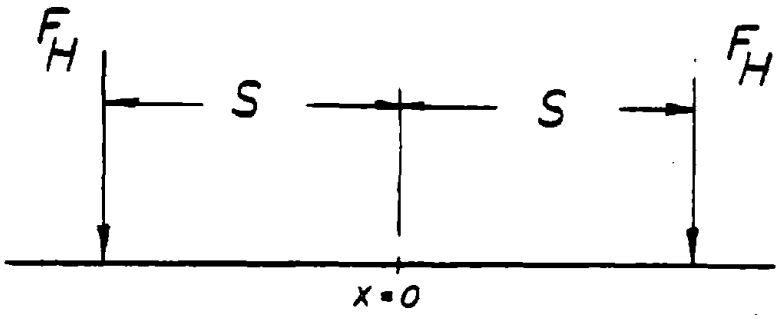

FIGURE B.1 - LATERAL LOADS IN TRUCK LOAD CASE

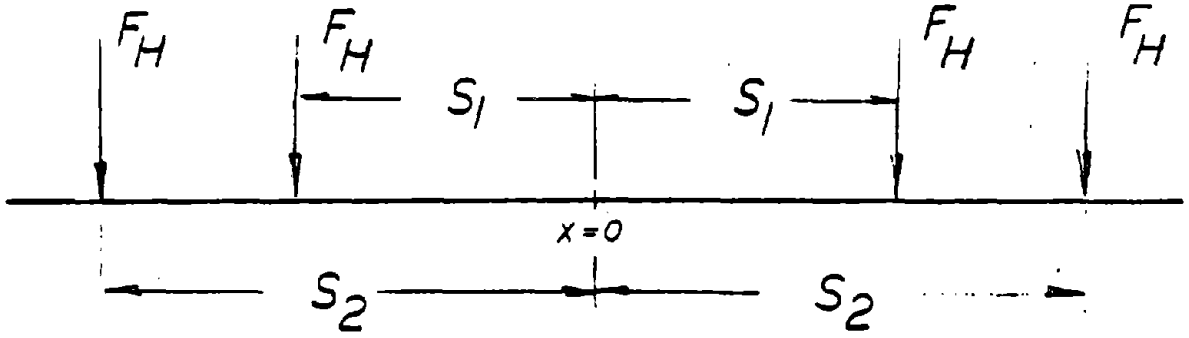

FIGURE B.2 - LATERAL LOADS IN VEHICLE LOAD CASE

Vehicle Load Case

$$a_{m3} = \begin{cases} 0 & \text{for } L \leq S_1 \\ -\frac{2F_H}{L} \cos\left(\frac{m\pi S_1}{2L}\right) & \text{for } S_1 < L \leq S_2 \\ -\frac{2F_H}{L}\left[\cos\left(\frac{m\pi S_1}{2L}\right) + \cos\left(\frac{m\pi S_2}{2L}\right)\right] & \text{for } L > S_2 \end{cases} \qquad \text{(B-20.3)}$$

It should be noted that in all cases considered symmetry has been assumed. Therefore, the center of the buckled wave shape occurs midway between the applied loads for a multiple load case or directly at the point of load application for a single load case.

Correction for Change in Longitudinal Resistance

In the foregoing analysis, the change in the track longitudinal resistance due to vertical wheel loads has not been considered. Clearly the longitudinal resistance is decreased in the lift off region and significantly increases directly under the load. To be rigorous we shall employ the same Hetenyi analysis as used in the lateral resistance evaluation for the determination of the longitudinal resistance. We recall that the longitudinal resistance in the buckling zone is neglected in the analysis and also that its influence on the buckling temperature is minimal [4]. In view of these considerations, an approximate correction for the effect of changed longitudinal resistance due to wheel loads is proposed. It is assumed that the increase in resistance equals μV_t concentrated at the truck center (where μ = friction coefficient, V_t = total vertical truck load.) The rail force before and after buckling is shown in Figure B-3.

Let u = longitudinal displacement in the buckling zone

$$U_1 = \frac{f_o x^2}{2EA} + C_1 X + C_2 \text{ in the breathing zone 1}$$

$$U_2 = -\frac{f_o x^2}{2EA} + C_3 X + C_4 \text{ in the breathing zone 2}$$

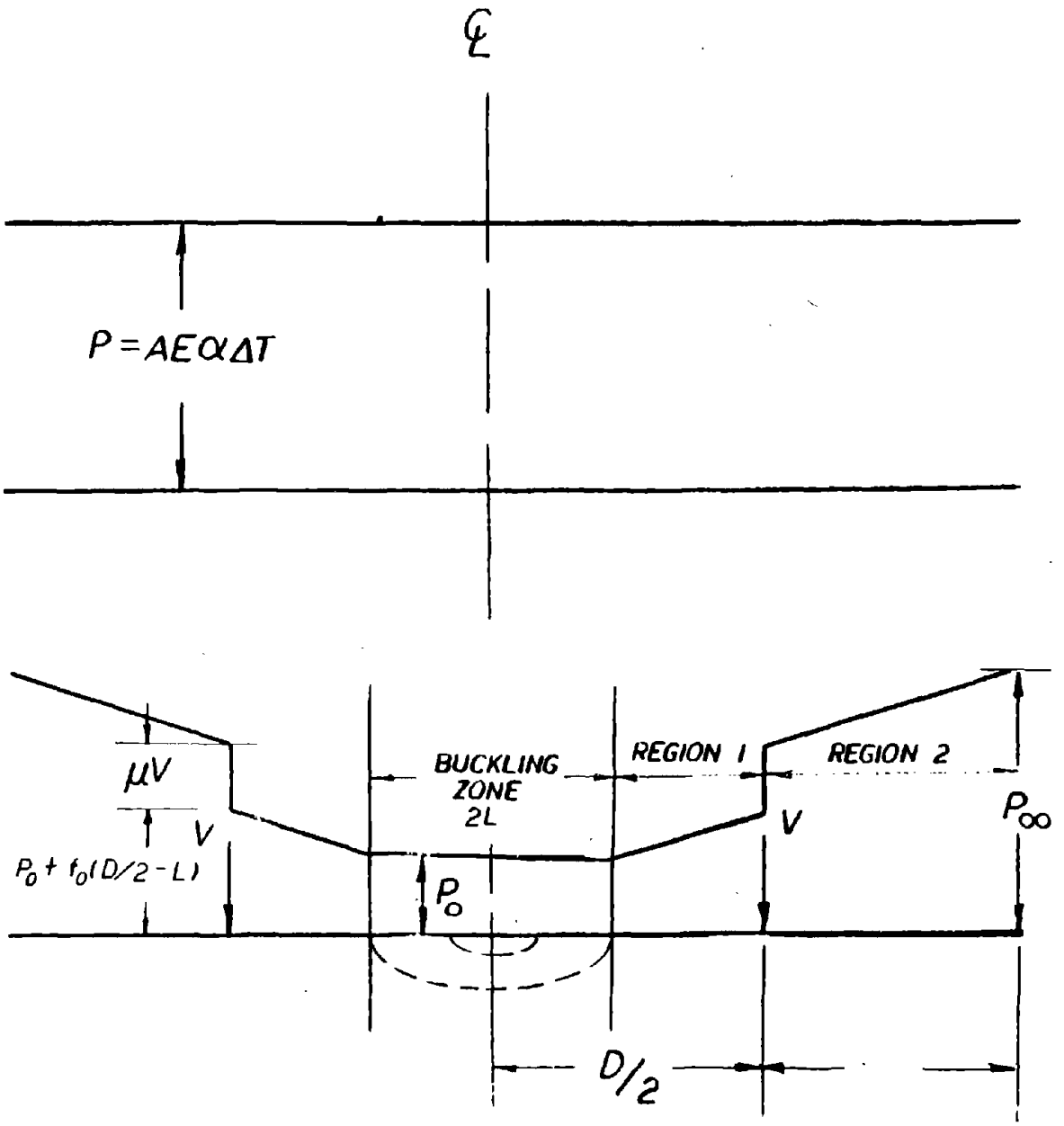

FIGURE B.3. FORCE DISTRIBUTION BEFORE AND AFTER BUCKLING

The continuity and the boundary conditions are:

At $x = D/2$

$$U_1 = U_2 \tag{B.21}$$

$$AE(U_1' - U_2') = \mu V_t \tag{B.22}$$

At $x = L$

$$u = U_1 \tag{B.23}$$

$$u' = U_1' \tag{B.24}$$

At $X = \ell_\infty$

$$U_2 = 0 \tag{B.25}$$

$$U_2' = 0 \tag{B.26}$$

From the previous work [2], we know that

At $x = L$

$$u = -\frac{\bar{P}L}{EA} - Z + \alpha TL \tag{B.27}$$

$$u' = -\frac{\bar{P}}{EA} + \alpha\bar{T} \tag{B.28}$$

Using these equations, we find that

$$\ell_\infty = L^2 + 2\,EAZ/f_o - \mu V_t D/f_o \tag{B.29}$$

and

$$T = \frac{\bar{P}}{AE\alpha} + \frac{Lf_o}{AE\alpha}\left\{-1 + \sqrt{1 + \frac{2AEZ}{f_o L^2} - \frac{\mu V_t D}{f_o L^2}}\right\} + \frac{\mu V_t}{AE\alpha} \tag{B.30}$$

Note that the correction for "dynamic" longitudinal resistance in (B-30) is through the terms containing V_{t_1}, and taking $\mu V_t = 0$ yields the static case (Equ. B-6.1).

REFERENCES

1. Kerr,A.D., "Analysis of Thermal Track Buckling in the Lateral Plane," Princeton University, September 1976, DOT/FRA/ORD-76/285, NTIS PB267938.

2. Samavedam,G., "Buckling and Post Buckling Analyses of CWR in the Lateral Plane," British Railways Board, R&D Division, Technical Note TN-TS-34 (January 1979).

3. Kish,A., G. Samavedam, and D. Jeong, "Analyses of Thermal Buckling Tests on U.S. Railroads," Transportation Systems Center, November 1982, DOT/FRA/ORD-82/45, NTIS PB83 203554.

4. Samavedam,G., A. Kish and D. Jeong, "Parametric Studies on Lateral Stability of Welded Rail Track," Foster-Miller, Assoc., May 1983, DOT/FRA/ORD - 83/07, NTIS PB83 215517

5. Kish,A., and G. Samavedam, "Recent Investigations on Lateral Stability of Continuous Welded Rail Track," American Railway Engineering Association Bulletin 688, Vol. 83 (1983) pp. 565-594.

6. Zarembski,A.M., and G. Magee, "An Investigation of Railroad Maintenance Practices to Prevent Track Buckling," AAR Report # R-454 (November 1980).

7. Nagy,J., "Experimental Investigations on CWR Track Behavior Due to Thermally Induced Loads, V" (1970) Yearbook of the Hungarian Railway Scientific Research Institute, in Hungarian.

8. Nagy,J., "Experimental Investigations on CWR Track Behavior Due to Thermally Induced Loads, VI," (1974) Yearbook of the Hungarian Railway Scientific Research Institute, in Hungarian.

9. Sonneville,R., and A. Bentot, "Elasticite et resistance laterale de la voie," Monthly Bulletin of the Interanational Railway Congress Assoc. (November 1953).

10. Amans,F., and R. Sauvage, "Railway Track Stability in Relation to Transverse Stresses Exerted by Rolling Stock, A Theoretical Study of Track Behavior," Annales des Ponts et Chaussees, No. 1 (Jan - Feb 1969), in French.

11. Frederick,C.O., "The Effect of Lateral Loads on Track Movement," British Railways Board, R&D Division, Technical Note TN-TS-4 (January 1973).

12. Bolotin,V.V., Dynamic Stability of Elastic Systems (Holden-Day, Oakland, 1964).

13. Hetenyi,M., Beams on Elastic Foundation (University of Michigan, Ann Arbor, 1946).

14. Kish,A., G. Samavedam, and D. Jeong, "Effect of Vertical Imperfection on Lateral Stability of CWR," (in preparation).

15. Eastern European Track Structure Technology and Research, FRA/ORD - 81/58 (July 1981).

16. Kerr,A.D. and S. B. Bassler, "Effect of Rail Lift-off on the Analysis of Railroad Tracks," National Science Foundation Report, Civil and Mechanical Engineering Division, Structural Mechanics Program, Research Report CE-80-19 (October 1980).

17. Eisenmann,J., "The Significance of the Rail Lifting Wave," Rail International, No. 10 (October 1976), pp. 576-581.

18. Kish,A., and G. Samavedam, "Test Requirements Definition for Dynamic Buckling Tests," Transportation Systems Center Project Memorandum, (December 1982).

19. Dogneton,P., "The Experimental Determination of the Axial and Lateral Track Ballast Resistance," Railroad Track Mechanics and Technology, Proceedings of a symposium held at Princeton University, April 21-23, 1975, edited by A.D. Kerr (Pergamon Press, 1978).

20. ORE Committee D117, "Influence of Various Measures on the Lateral Displacement Resistance of the Unloaded Track," DT44/D117/D (1976).

21. Ghadiali,N. and T. Wall, "Analysis of Track Uplift," Battelle Columbus Laboratory Report, prepared for Transportation Systems Center, Contract No. DTRS-57-83C-00076 (1983).